# ROLE OF GCN2 IN GUIDING THE CELLULAR AND MOLECULAR RESPONSE TO ASPARAGINASE IN THE PANCREAS

By

LINDSEY PHILLIPSON-WEINER

A thesis submitted to the

Graduate School-New Brunswick

Rutgers, The State University of New Jersey

in partial fulfillment of the requirements

for the degree of

Master of Science

Graduate Program in Nutritional Sciences

written under the direction of

Dr. Tracy G Anthony

And approved by

_____

_____

_____

New Brunswick, New Jersey

October 2015

ABSTRACT OF THE THESIS

Role of GCN2 in Guiding the Cellular and Molecular Response to Asparaginase in the Pancreas

By LINDSEY PHILLIPSON-WEINER

Thesis Director:

Dr. Tracy G Anthony

Asparaginase is a chemotherapy agent used in the treatment of acute lymphoblastic leukemia. Asparaginase can cause severe pancreatitis but the molecular basis is unknown. In liver of mice, the eIF2 kinase GCN2 is essential for mitigating metabolic stress caused by asparaginase. This study examined the role of GCN2 in the pancreas of mice treated with asparaginase. Eight week old wild type or GCN2 KO mice were injected once daily for 8 d with either 3 IU/g BW of saline or asparaginase. Eight hours after final injection, mice were sacrificed and pancreata were weighed and harvested. In GCN2 KO mice treated with asparaginase, pancreas weights were significantly increased ($P<0.05$) and the organs visibly enlarged. Histological examination revealed ductal dilatation and swollen acinar cells in GCN2 KO only. Oil red O staining and measurement of pancreas triglycerides ruled out lipid accumulation as a contributing factor. No signs of cell death by TUNEL stain were detected in the pancreas, and serum amylase activity did not differ among treatment groups. However, Pancreatitis Associated Protein (PAP) mRNA expression was elevated in livers of

asparaginase-treated GCN2 KO mice only. Phosphorylation of eIF2 and pancreatic expression of asparagine synthetase were similar among treatment groups, but mTORC1 signaling was decreased to the greatest extent in the pancreata of asparaginase-treated GCN2 KO mice. Additionally, transmission electron microscopy revealed evidence of ER stress in GCN2 KO mice treated with asparaginase. These data suggest that loss of GCN2 predisposes the pancreas toward the development of asparaginase-associated pancreatitis. NIH HD070487

# ACKNOWLEDGMENTS

I express my sincere gratitude to my advisor and mentor, Dr. Tracy Anthony. Thank you for supporting me and helping me find my way. Your knowledge and endless passion for your work is something that I hope to emulate in my future career. Thank you for your guidance and advice throughout my research project. Your love of amino acids is infectious, and I am so thankful for the opportunity to work in your lab. I am extremely appreciative for your support when I decided to change career paths and switch over to the “dark side.” I would like to acknowledge and thank my committee members, Dr. Malcolm Watford and Dr. Geoff McAuliffe, for their advice, encouragement, and support.

I would like to thank Sarah Hassenain and Juliet Gotthardt for helping me to not fail out of graduate school, especially when I was crying every single day after first moving to New Jersey. Studying with you was the best and the worst, and I am happy that you were able to keep me on task/feed me. Maybe once I graduate I will learn how to correctly spell your last names. I would like to thank Anna Dinh for always being ready to take a snack break, and for taking my baby jokes so well. Also, thanks for the help and advice with the science.

I would not have been able to complete my project without the help of everyone from the Anthony Lab. Dr. Gabe Wilson, thank you for showing me how to do western blots and analyze PCR data and for teaching me that I can decipher hieroglyphics (just kidding it’s just your handwriting). I have to express my enormous appreciation for Emily Mirek. Thank you for loving mice and for

being the mouse whisperer, so that I don't have to risk getting bitten by them. I can't even begin to express how thankful I am that you were lab manager of the lab. Thank you for all of your work that is so vital and at the heart of keeping our lab functional. Rana Al-Baghdadi, I am so happy that we joined the lab around the same time. I am so appreciative for having you as a fellow graduate student during my time in the lab. You are so smart, and so capable, and I am always so amazed with how you manage to do it all. Thank you to Dr Inna Nikonorova, without your magic touch, I might still be trying to isolate high quality RNA from the pancreas. Thank you Dr Yongping Wang for helping me troubleshoot various projects, I learned so much from our troubleshooting experience. Thank you Dr Ashley Pettit for always feeding me! Thank you to the methionine restriction boys, Albert Bargoud, Berish Wetstein and William Johnson. Some of my favorite lab memories are with you guys. Thank you to our other undergraduate students Matthew Solowsky, Brittany Leigh Lennox and Casey Fannell for doing all of the menial tasks, for maintaining an efficient workspace, helping with my experiments, and of course being great company.

I have met some incredible people here at Rutgers, who have offered me such great advice and are always there for a much needed vent session. Many thanks to Bryn Yeomens, Atreju Lackey, Marc Tuazon and the community crew, Pamela Barrios, Fanfan Wu and Kati Beluska for all of the advice, support and laughs. I would also like to thank the rest of the graduate students in the Nutritional Sciences department here at Rutgers. I would also like to thank my Puerto Rican grandmother, Carmen Acevedo. Your loving and caring nature was

probably why I finally stopped crying every single day. I am also incredibly fortunate to have the greatest friends; thank you to everyone who tolerated my boring science discussions, busy hours, and inability to talk about anything other than what I am learning.

Finally, I'd like to thank my family who believe in me when they probably shouldn't. You guys are my rock and I am eternally grateful for all that you guys have done for me. Thank you Dad for nerding out with me and boring everyone in the general vicinity. Thank you Mom for endless mommying and discussion of all things clinical. Thank you to my sisters, Rebecca and Elizabeth for falling asleep when I talk about my research and helping me craft my sentences in an attempt to try and make you two losers understand. Also, thank you for always making me laugh and not judge me when I am being my weirdest. I love you guys more than I could ever possibly articulate and I thank you for all of your support when I became a Jersey Girl.

# TABLE OF CONTENTS

# LIST OF FIGURES

# LIST OF ABBREVIATIONS

4E-BP1- eIF4E Binding Protein 1

AAP-Asparaginase Associated Pancreatitis

AAR-Amino Acid Response

Akt-Protein Kinase B

ALL- Acute Lymphoblastic Leukemia

ASNase- Asparaginase

ASNS-Asparagine Synthetase

ATF3-Activating Transcription Factor 3

ATF4-Activating Transcription Factor 4

ATF5-Activating Transcription Factor 5

ATF6- Activating Transcription Factor 6

B6J-C57 Black 6 Jackson

BiP-B cell immunoglobulin protein

BW-Body weight

CHOP/GADD153-C/EBP Homologous Protein

C/EBPβ– CCAAT/enhancer binding

DTT- Dithiothreitol

EDTA- Ethylenediaminetetraacetic acid

EGR1-Early Growth Response 1

eIF2-Eukaryotic Initiation Factor 2

eIF4E-Eukaryotic initiation factor 4E

ER-Endoplasmic Reticulum

ERAD-Endoplasmic reticulum associated protein degradation

ERK1/2-Extracellular signal regulated kinase

FGF21-Fibroblast growth factor 21

FMOC-9-fluorenylmethyl chloroformate

FSR-Fractional synthesis rate

GA- GCN2$^{-/-}$ Asparaginase

GCN2-General Control Nonderepressible 2

GP-GCN2$^{-/-}$ PBS

Grp78-Glucose regulatory protein 78

HCl-Hydrochloric Acid

HEPES- 4-(2-hydroxyethyl)-1-piperazineethanesulfonic acid

HPLC-High performance liquid chromatography

HRI-Heme regulated inhibitor

IRE1- Inositol requiring 1

ISR-Integrated Stress Response

IU-International Units

JNK-cJUN N terminal Kinase

KCl-Potassium Chloride

KO-Knock out

LCMS-Liquid chromatography mass spectroscopy

LiCL-Lithium Chloride

MID-Medication induced diabetes

mTOR-Mammalian/Mechanistic target of rapamycin

mTORC1-Mammalian/Mechanistic Target of Rapamycin Complex 1

NaCl – Sodium chloride

NaF – Sodium fluoride

NaOH-Sodium Hydroxide

OPA-Ortho-phthalaldehyde

p-eIF2-Phosphorylation of the alpha subunit of eIF2

P70S6K- Ribosomal p70 S6 Kinase

PAP-Pancreatitis associated Protein

PBS – Phosphate buffered saline

PCA-Perchloric Acid

PCR-Polymerase Chain Reaction

PERK-PKR-like ER-resistant Kinase

PI3K-Phosphoinositide 3 Kinase

PKR-RNA dependent protein kinase

PMSF- Phenylmethanesulfonylfluoride

PRAS40- Proline-rich AKT substrate

PPARG-Peroxisome proliferator activated receptor gamma

PVDF-Polyvinylidene difluoride

Rheb- Ras homolog enriched in brain

RIPA-Radioimmunoprecipitation Assay

SDS – Sodium dodecyl sulfate

SIRT1-Sirtuin 1

SNP-Single nucleotide polymorphism

sXBP1-Spliced XBox Binding Protein 1

T2D-Type 2 Diabetes

TBST – Tris buffered saline with Tween-20

TNFα- Tumor Necrosis Factor alpha

TSC1- Tuberous Sclerosis 1

TSC2- Tuberous Sclerosis 2

ULK- UNC-5 like autophagy activating complex

UPR-Unfolded Protein Response

uXBP1-unspliced X-Box Binding Protein 1

WA-Wildtype Asparaginase

WP-Wildtype PBS

WRS- Wolcott-Rallison Syndrome

WT – Wild-type

XBP1-XBox Binding Protein 1

# INTRODUCTION

## Acute Lymphoblastic Leukemia

Acute lymphoblastic leukemia (ALL) is the most common form of childhood cancer with an incidence of 3-5 per 100,000 children in Europe and the United States (1,2). ALL is caused by unregulated proliferation of immature lymphocytes leading to neoplastic accumulation of lymphoblasts within bone marrow (3,4). Treatment regiments include multi-component chemotherapeutic agents. One of most commonly used agents in this drug cocktail is L-asparaginase, which has been in use as a chemotherapy agent to treat ALL since the 1960s (5,6). While asparaginase is very effective, contributing to current remission rates of 83-95% in patients (1), there are many negative side effects associated with treatment. The most severe side effects include thrombotic events, allergic reactions, hyperlipidemia, hepatotoxicity and pancreatitis (1,5–7). Asparaginase Associated Pancreatitis (AAP), the onset of acute pancreatitis following treatment with asparaginase, occurs in roughly 16% of treated patients (1,7,8). Clinically, AAP can present as abdominal pain, slight fever, nausea, severe abdominal tenderness as well as metabolic abnormalities such as hyperglycemia and diabetes (1,5,9). Accordingly, there is a 43.8% mortality rate in ALL patients who develop AAP (1,8). Furthermore, patients typically suffer from pancreatic enlargement, necrosis, and in severe cases pancreatic pseudocysts (1,9).

## Asparaginase

Asparaginase is a drug, which is used as a chemotherapy agent for treatment of different types of leukemic cancers. Asparaginase works by

catalyzing the hydrolysis of asparagine to yield aspartate (Figure 1), which ultimately depletes the body's pool of this non-essential amino acid. When utilized as a chemotherapy agent, the rationale is that certain tumor types are unable to synthesize asparagine due to low or absent levels of asparagine synthetase (ASNS) (10–13) and thus these tumors depend on circulating levels of asparagine to meet their metabolic needs. Since asparaginase, depletes the

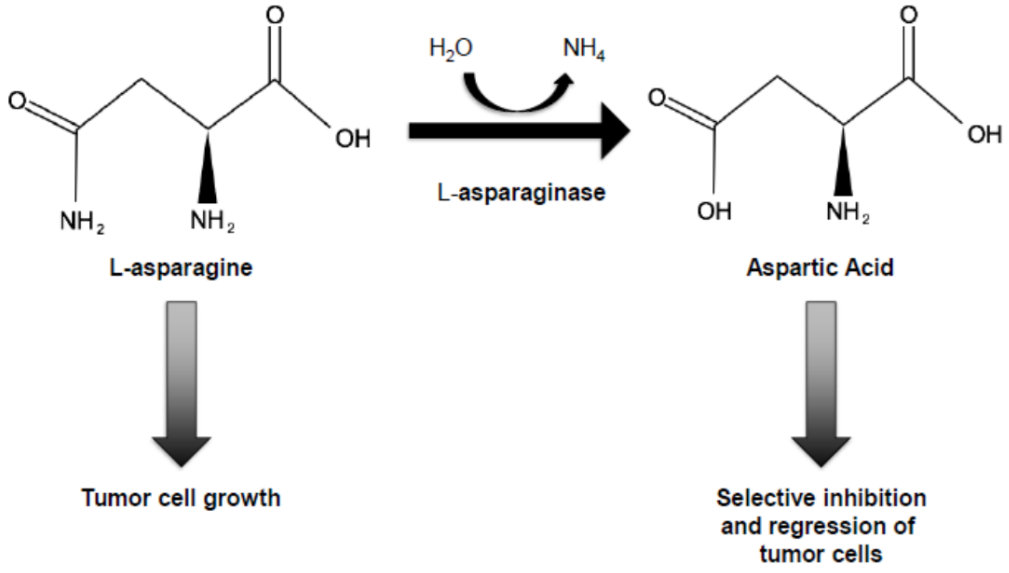


endogenous asparagine supply, the tumor will be unable to grow, leading to tumor cell death.

**Figure 1: Asparaginase Mechanism of Action.**
Asparaginase is a drug used to treat acute lymphoblastic leukemia. Lymphocytic leukemia cells lack the ability to synthesize asparagine and thus rely on the body pool. L-asparaginase catalyzes the conversion of L-asparagine to L-aspartate and ammonia depriving the leukemic cells of this essential amino acid and thus inhibiting growth. Figure adapted from El-Nagga *et al.,* 2014 Int. J. of Pharmacology, 10:182-199 (13)

Glutamine serves as a substrate for the synthesis of asparagine. Upon conversion of glutamine to glutamate, the free ammonia is used in the synthesis of asparagine from aspartate via ASNS (Figure 1). Thus, the ability of asparaginase to deaminate asparagine as well as glutamine is essential to starvation of the tumor to prevent protein synthesis (14). Many of the cytotoxic effects associated with asparaginase treatment are due to its secondary glutaminase activity (15). Reinert et al examined differences between using an *E.coli* derived asparaginase and *Wolinella* derived asparaginase and showed that only the *E.coli* derived enzyme reduced circulating levels of glutamine(15). The work by Reinert et al. further established that the *E.coli* derived asparaginase reduced liver protein synthesis as well as mTOR signaling compared to *Wolinella* which did not reduce either protein synthesis or mTOR signaling (15) suggesting that the glutaminase activity of the *E.coli* form contributes significantly to hepatic stress by asparaginase.

**Types of Asparaginase**

There are three drug forms of asparaginase; *E.coli* asparaginase, PEG-asparaginase and *Erwinia chrysanthemi* asparaginase. These forms of asparaginase can be administered intramuscularly or intravenously (16,17). The *Erwinia* form has a shorter half-life than the *E.coli* derived asparaginase and is delivered to patients at a higher dose (16,17). Pegylation of the *E.coli* L-asparaginase increases the half-life of the preparation significantly compared against the other two forms. Clinically, the pegylated form has a half-life of 5.7 ± 3.2 days (18,19) compared to the *E.coli* derived half like of 1.24 ± 0.17 days and

0.65 ± 0.13 days for the *Erwinia* derived asparaginase (20). In vivo, the half-life of *E.coli* derived asparaginase is approximately 5 hours compared to the *Erwinia* derived asparaginase which is approximately 10 hours and pegylated asparaginase which lasts approximately 20 hours (21). Pegylation also decreases the host anti-drug antibody response (17,22) and is often used if patients suffer from hypersensitivity reactions (18,20). Despite the difference in drug preparation, all forms of the drug elicit similar metabolic toxicities. While different forms of the drug offer multiple options for patients that experience toxicity, it is not clear how to predict which form is best for each individual patient. While, there are no gender differences with the development of metabolic toxicities following asparaginase treatment, there is an age effect with a greater incidence of toxicities occurring in older patients (7,8,23,24).

**Asparaginase Associated Pancreatitis**

The development of pancreatitis during asparaginase treatment can be very clear and dramatic. The onset of acute pancreatitis following treatment with asparaginase occurs in roughly 16% of treated patients (1,5,9). In a 5-year retrospective study examining the onset of AAP, pancreatitis was seen with administration of all three drug forms, and there were no differences between the number of doses administered and the development of AAP (7). There is a 43.8% mortality rate in ALL patients who develop AAP (9), however the exact mechanism precipitating this event unclear.

**Amino Acid Response Pathway**

The asparaginase-induced reduction in asparagine activates a specific protein kinase called general control nonderepressible 2 (GCN2, or EIF2AK4 in humans). GCN2 is highly conserved among eukaryotes and is expressed in simple organisms like yeast and complex organisms like humans. GCN2, is expressed in the majority of body tissues, including the immune system, nervous system, muscle, secretory, reproductive and internal organs. Despite abundant expression across tissues in mammals, whole body deletion of GCN2 does not appear to alter growth, fertility or lifespan in mice maintained with sufficient

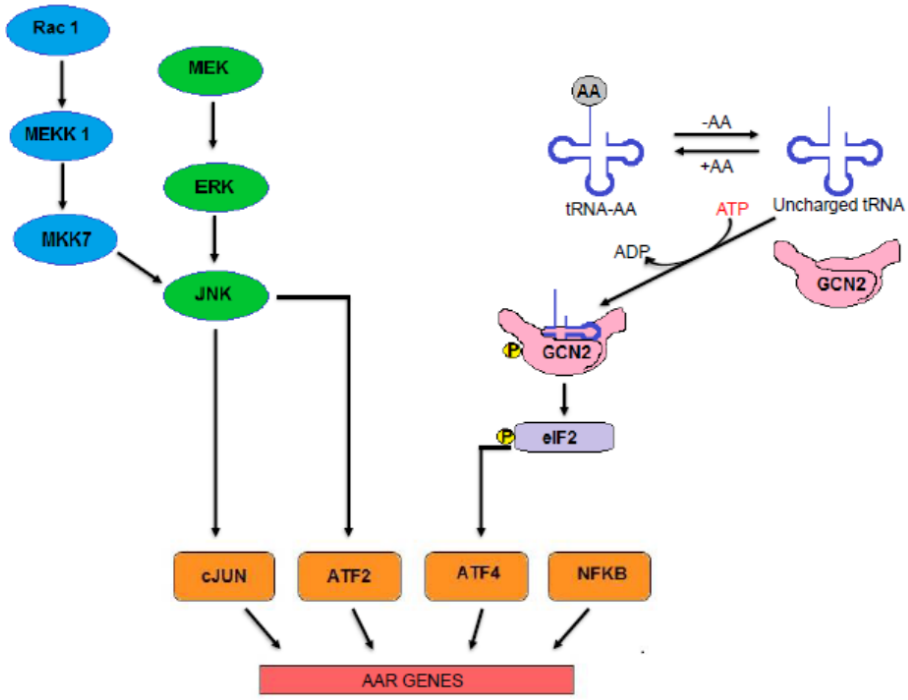


**Figure 2: Amino Acid Stress Response.**
Inadequate levels of an amino acid are sensed by GCN2. GCN2 activates a signal cascade by phosphorylating eIF2, which serves to alter gene expression patterns in an order to adapt to this amino acid stress. Figure adapted from Balasubramanian *et al.*, 2013 Am J Physiol Endocrinol Metab. 304(8):E789-99(25).

supplies of all amino acids. However, upon amino acid insufficiency GCN2 is activated, phosphorylating eukaryotic initiation factor 2 (eIF2), which decreases general protein synthesis while simultaneously increasing translation of specific mRNAs (Figure 2). This effort to regain protein homeostasis through altered protein synthesis and subsequently gene expression is coined the Amino Acid Response (AAR) by Kilberg and colleagues (25). Primary signaling through the AAR occurs via GCN2; however, an additional component of the AAR is signaling through the MEK/ERK pathway, which also serves to alter the transcriptome. Ultimately, activation of the AAR serves to promote homeostasis and cell survival.

**Activation of GCN2**

There are four eIF2 kinases, each which phosphorylate eIF2 in response to specific types of environmental stressors (Figure 3); PERK (PKR-like ER-resistant Kinase) which is activated in response to misfolded proteins and ER stress, PKR (RNA dependent protein kinase) which responds to dsRNA and is involved in viral defense mechanisms and HRI (heme-regulated inhibitor) which responds to heme deprivation or heat shock stress (2). GCN2 is the oldest and most highly conserved of these kinases and is found in a variety of species ranging from yeast to mammals (26).

Deprivation of a single amino acid results in the accumulation of uncharged tRNA within the cell (15,27). GCN2 senses reductions in aminoacylated tRNA by binding uncharged tRNA in a region with structural homology to histidinyl tRNA synthetase,

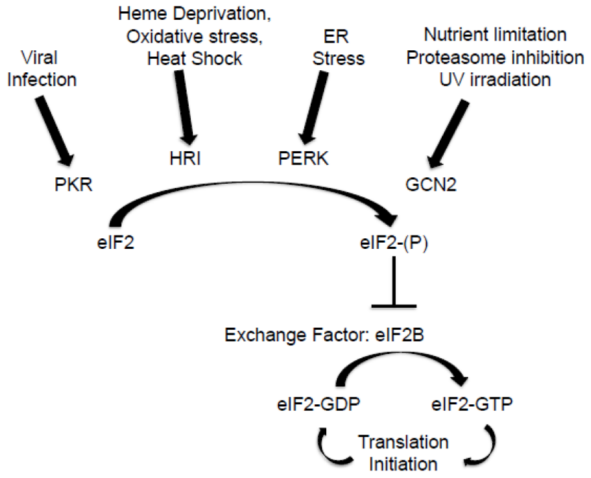


**Figure 3: Activation of eIF2 kinases**
Figure adapted from Wek et al. 2006. *Biochem Soc Trans*.34:7-11 (2).

causing dimerization and auto activation of kinase activity directed toward eukaryotic initiation factor 2 (26,28). Phosphorylation of the alpha subunit of eIF2 (p-eIF2) at serine-51 position via GCN2 is an essential adaptation to amino acid stress resulting in a reduction of general protein synthesis and an increase in gene-specific translation of transcription factors such as Activating Transcription Factor 4 (ATF4). When GCN2 is inactive, eIF2 is bound to GTP and aids in initiation of protein synthesis by delivering methionyl tRNA to the ribosome. Once this delivery is complete, eIF2 bound to GDP is recycled back to its GTP bound form via the guanine nucleotide exchange factor eIF2B (2,28,29) ATF4 is preferentially translated in response to amino acid stress, and aids in the global reduction of protein synthesis by increasing mRNA expression of eIF4E binding protein 1 (4E-BP1). 4E-BP1 serves as the translational inhibitor of protein synthesis by blocking association of eIF4E with eIF4G and reducing assembly of the eIF4F complex (30,31) and thus blocking initiation of mRNA translation. ATF4

also up-regulates expression of genes that help to alleviate oxidative stress and activates additional cytoprotective pathways (32). Proteins encoded by these genes are involved in antioxidant defense, cell cycle arrest, and other molecular chaperones (33). Activation of the AAR by GCN2 mediated phosphorylation of eIF2 is essential for the adaptation to the amino acid starvation induced by asparaginase (27). However if the amino acid stress is too much for the cell to handle, the cell will alter its transcriptional profiles and will switch from increasing translation of cell survival proteins to promoting apoptosis and cell death related proteins such as C/EBP Homologus Protein (CHOP/GADD153) (34).

**FGF-21**

Fibroblast growth factor-21 (FGF21) is a target gene for ATF4 and CHOP and amino acid deprivation has been shown to induce FGF21 expression (35). FGF21 is produced predominantly by liver and acts as a metabolic hormone. It is also produced by other tissues involved in lipid metabolism and glucose regulation such as pancreas, adipose tissue and skeletal muscle (36,37). Studies show that FGF21 may be integral in cellular adaptation to nutritional stress. In response to nutrient deprivation, increased FGF21 expression has been shown to increase lipolysis in adipose tissue, allowing the conversion of fatty acids within the liver to be converted to ketone bodies as utilized as an energy source (35). Additionally, PPARα induces FGF21 which results in increased lipid oxidation and ketogenesis (38).

In the pancreas, FGF21 may serve a protective function in beta cells. FGF21 is an important regulator of glucose homeostasis. Presence of this

hormone aids in glucose uptake by adipocytes, has been shown to lower both blood glucose and triglyceride levels in diabetic mice (39). Additionally, FGF21 signaling through the ERK1/2 pathway was protective against beta-cell apoptosis and also helped increased insulin secretion from diabetic islet cells (37,40). Thus the presence of FGF21 may be protective in times of cellular stress.

**MTOR pathway**

Inhibition of global protein synthesis by asparaginase occurs through GCN2 activation of the AAR and inhibition of the mammalian/mechanistic target of rapamycin complex 1 (mTORC1) signaling pathway. mTOR is a member of the serine/threonine kinase family and is activated in times of nutrient abundance. mTOR is composed of two sub-complexes called, mTORC1 and mTORC2. Activation of mTORC1 occurs through growth factors such as insulin, and activation of this complex results in anabolic growth, cell survival and metabolism (41–43). The molecular mechanism of activation (Figure 4) begins with phosphoinositide 3-kinase (PI3K) activation of AKT, which promotes the action of mTORC1. AKT activation prevents proline-rich AKT substrate (PRAS40) from interacting with mTORC1 as well as phosphorylating and thus inactivating tuberous sclerosis 2 and 1 (TSC2-TSC1) which allows for the activation of Ras homolog enriched in brain (Rheb) (42,43). TSC1-TSC2 serves to prevent mTORC1 activation by maintaining Rheb bound to GDP, the inactive form. When Rheb is bound to GTP following growth signal stimulation of AKT, Rheb will stimulate mTORC1 kinase activity (41,42). Upon stimulation by the presence of amino acids, mTORC1 will migrate to the surface of the lysosome, which is mediated by the raptor component of this complex. Negative regulation

of mTORC1 occurs by signaling through TSC1-TSC2. An energy deficit, lack of oxygen and genotoxic stress positively activate TSC1-TSC2 which will inhibit mTORC1 signaling (41).

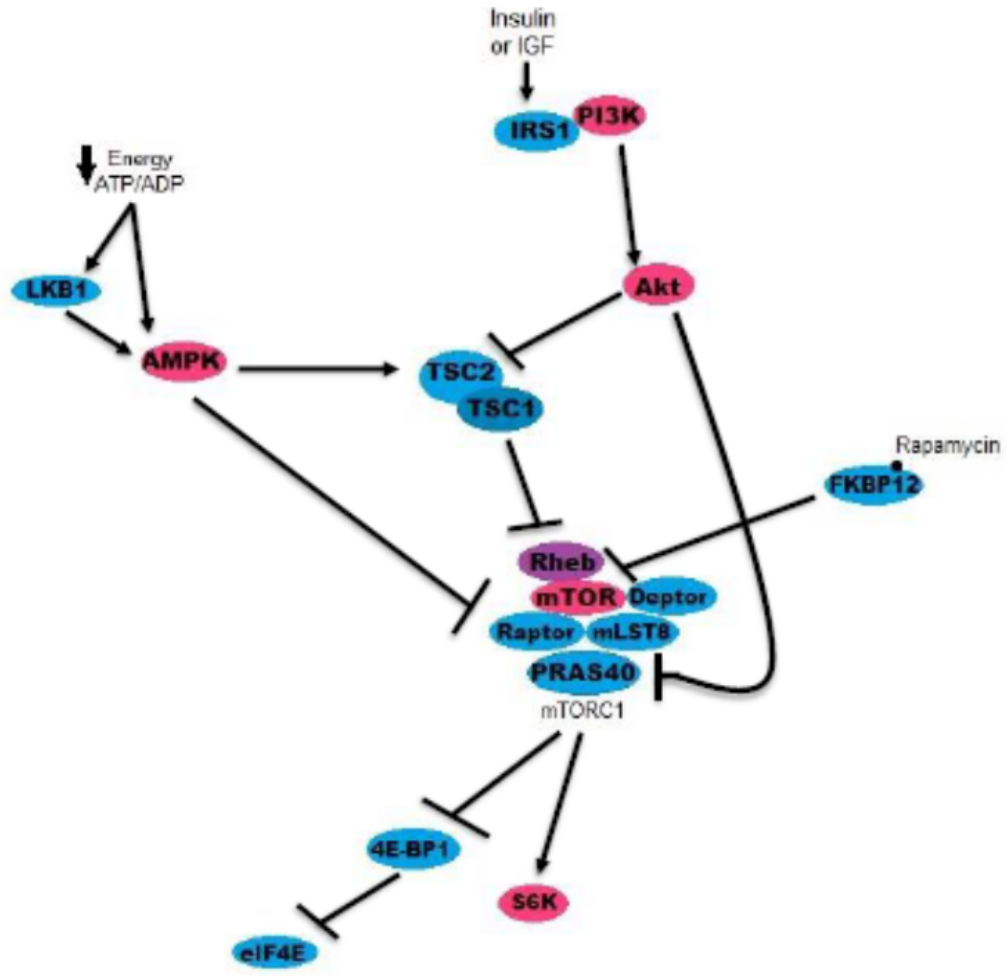


**Figure 4: PI3-Akt-mTOR Pathway Activation**
Activation of the PI3 kinase pathway and its downstream effectors in response to nutrient sufficiency. Downstream signaling of Akt through mTOR to either supress or promote protein synthesis and cellular proliferation. Figure adapted from Laplante, M. and Sabatini, D.*, 2012* Cold Spring Harb Perspect Biol. 4(2):a011593 (41)

In times of nutrient sufficiency, signaling through mTORC1 occurs to stimulate cell growth and proliferation. Upon activation, mTORC1 phosphorylates

ribosomal p70 S6 Kinase (p70S6K) and eukaryotic translation initiation factor 4E (eIF4E) and its associated binding proteins (4EBP1). eIF4E is a member of the multi-subunit complex which aids in the recruitment of the 43S ribosomal complex to the mRNA strand to begin translation (44). Phosphorylation by mTORC1 of 4EBP1 leads to the dissociation of 4EBP1 from eIF4E, which promotes the assembly of eIF4E with eIF4G (45,46). The association of eIF4E with eIF4G allows for the mRNA to bind to the 43S and begin translation. In times of nutrient deprivation, 4EBP1 is not phosphorylated, and thus remains associated with eIF4E preventing translation.

mTOR also plays a role in the activation of autophagy. Autophagy is the cellular recycling process that removes damaged organelles and macromolecules and recycles undamaged organelles. Autophagy induction occurs under conditions of low cellular energy and resources, conditions which inhibit mTORC1 signaling. When mTORC1 is active, it inhibits autophagy activation by phosphorylating UNC-5 like autophagy activating complex1/2 (ULK1/2) which inhibits the autophagy initiating complex, ULK (47). The activation of mTORC1 thus directly opposes the activation of autophagy.

**Asparaginase Activates the GCN2-eIF2-ATF4-AAR in Liver**

Treatment with asparaginase causes hepatotoxicity (Figure 5). Using *E.coli* derived asparaginase and *Wolinella* derived asparaginase, our laboratory showed differences in tissue specific responses to the nutrient stress. Only the *E.coli* derived asparaginase reduced liver and spleen protein synthesis, but did not alter pancreatic protein synthesis, compared to *Wolinella* derived

asparaginase which did not reduce protein synthesis in any tissues (15). This study showed that the amino acid stress induced by asparaginase is aggravated by the depletion of glutamine. Despite reduced circulating depletion of glutamine by the *E.*coli derived asparaginase, both asparagine and glutamine concentrations were unchanged in the pancreas (15). Further, no differences were noted in the phosphorylation of eIF2 in the pancreaseven though *E.coli* asparaginase elicited elevated ASNS mRNA in this tissue (15).

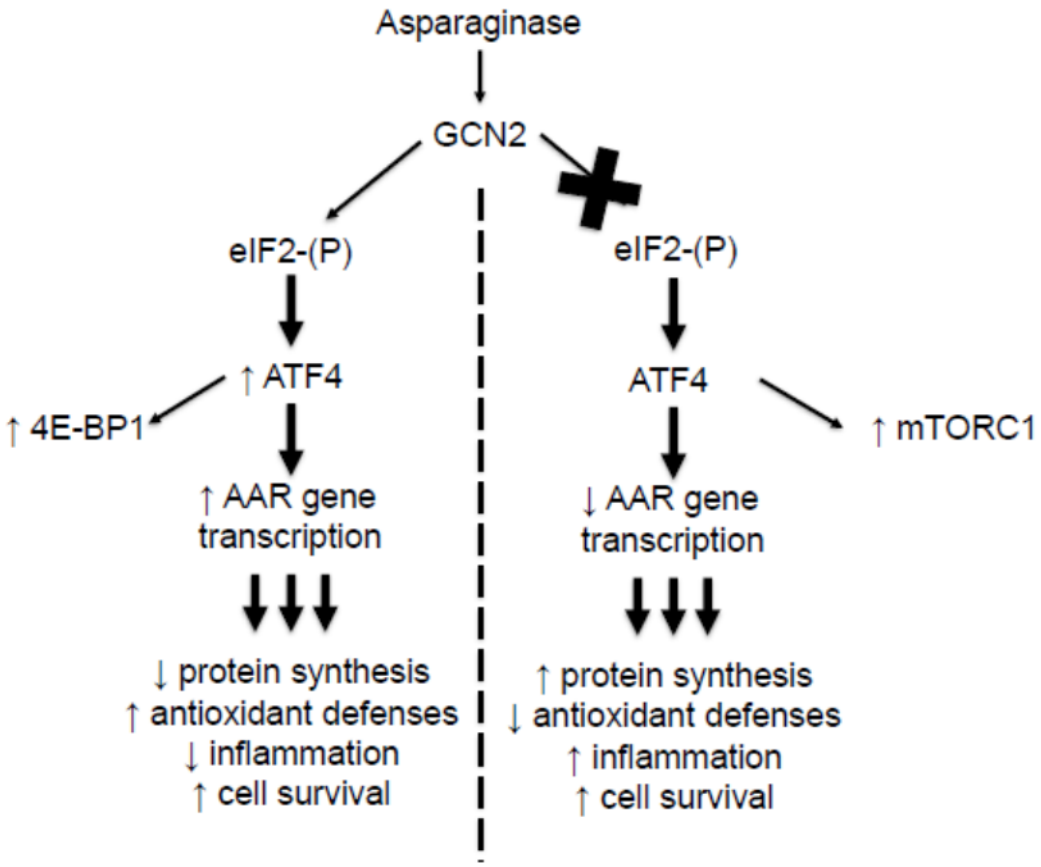


**Figure 5: Asparaginase Activation of GCN2.**
Asparaginase activation of the AAR in Liver. In the presence of GCN2, cellular adaptation occurs via signalling through eIF2. In the absence of GCN2, failure to activate the AAR via phosphorylation of eIF2 leads to hepatotoxicity.Figure adapted from Wilson *et al.,*2013. Am J Physiol Endocrinol Metab:305:E1124-E1133 (48).

Our laboratory previously reported that hepatic phosphorylation of eIF2 was increased in $GCN2^{+/+}$ animals treated with asparaginase as well as mice with a liver specific PERK deletion, however eIF2 phosphorylation did not occur in the livers of either $GCN2^{-/-}$ mice or mice with both GCN2 and PERK deleted in liver (27). This finding was the first to indicate the involvement of GCN2 in modulating the amino acid stress associated with asparaginase treatment. A single injection of asparaginase reduced phosphorylation of S6K1 and 4EBP1 in mice with intact GCN2 (27). Additionally, there was no difference in phosphorylation of eIF2 in the pancreas of $GCN2^{+/+}$ or $GCN2^{-/-}$ animals following a single asparaginase injection (27).

Furthermore, this laboratory has shown the importance of GCN2 in regulating the hepatic complications associated with asparaginase treatment (Figure 4). In wildtype animals treated with asparaginase, phosphorylation of eIF2 was observed as well as increased mRNA expression of target genes such as ATF4, ASNS, 4EBP1 and CHOP (48) within the liver. This protective response of the liver was blunted in $GCN2^{-/-}$ animals which received asparaginase treatment. Additionally, $GCN2^{-/-}$ animals exhibited hepatic increases in triglyceride accumulation, mTOR signaling as well as markers of oxidative stress and inflammation (48).

Most recently, this laboratory has reported a mechanism of AAR induction to alleviate the hepatic lipid accumulation seen in $GCN2^{-/-}$ animals that receive asparaginase treatment. This study showed an increase in circulating FGF21 concentrations in $GCN2^{+/+}$ animals but not $GCN2^{-/-}$ animals treated with

asparaginase (49). Genes involved in lipid synthesis were similarly reduced in both liver and white adipose tissue. ApolipoproteinB-100 was significantly reduced in GCN2$^{-/-}$ liver, suggesting the mechanism for impaired lipid metabolism in these animals upon treatment with asparaginase (49). These studies were the first to show the mechanism of hepatotoxicity that occurs in the absence of GCN2 under asparaginase treatment.

Our laboratory has reported that in the pancreas, neither *E.coli* derived asparaginase nor *Wolinella* derived asparaginase altered pancreatic protein synthesis. Additionally, pancreatic amino acid levels of glutamine and asparagine did not differ (15). This same study reported that there were no differences in the phosphorylation of eIF2, with asparaginase derived from difference sources. However, wildtype mice that received a single injection of *E.coli* asparaginase from this study showed elevated ASNS mRNA in the pancreas (15). In a follow up study, our lab showed that there was no difference in phosphorylation of eIF2 in the pancreas of GCN2$^{+/+}$ or GCN2$^{-/-}$ animals following a single asparaginase injection (27). Additionally, a single injection of asparaginase reduced phosphorylation of S6K1 and 4EBP1, in the pancreas of GCN2$^{+/+}$ but not GCN2$^{-/-}$ animals. This study also showed no change in phosphorylation of AKT in the pancreas of GCN2$^{+/+}$ or GCN2$^{-/-}$ mice (27). Phosphorylation of ERK1/2 was increased in the pancreas of animals with intact GCN2.

**Unfolded Protein Response: ER Stress**

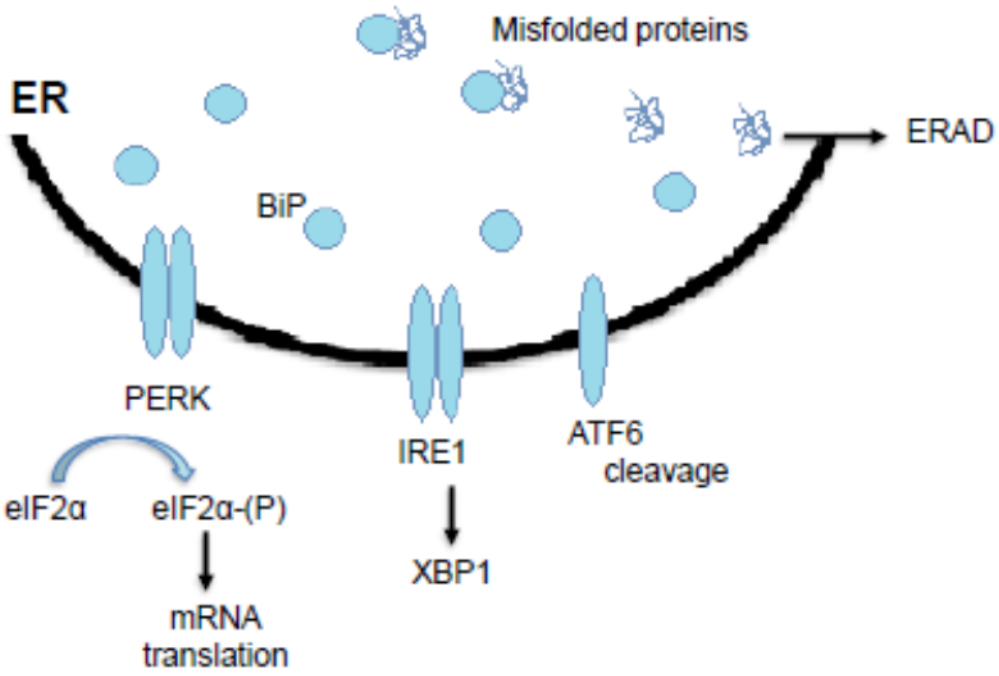


**Figure 6: The Unfolded Protein Response**
Schematic representation of activation of the unfolded protein response due to ER stress. Figure adapted from Julier, C. and Nicolino, M. *2010*. Orphanet Journal of Rare Diseases.5:29 (50)

The ER is responsible for synthesis, folding, trafficking and secretion of proteins within the cell as well as lipid synthesis and modification. Research shows that excess protein accumulation within cells is toxic, and many chronic diseases result from this cellular dysfunction and the resulting cell death (e.g., diabetes, cardiovascular disease, Alzheimer's disease) (51). If the ER stress is too much for the cell to handle, it will activate the UPR (52). Activation of the UPR (Figure 6) aims to restore homeostasis to the cell in the same way as the

AAR by decreasing general protein synthesis and simultaneously activating a signaling pathway to increase molecular chaperones as well as degrading misfolded proteins via ERAD (33,53,54). If the ER stress cannot be alleviated, then the UPR will switch to promoting apoptotic pathways.

UPR activation depends on three transmembrane proteins: Activating Transcription Factor 6 (ATF6), Inositol requiring 1 (IRE1) and PERK. Under normal non-stressed circumstances, a molecular chaperone, glucose regulatory protein 78, Grp78 (also known as B cell immunoglobulin protein (BiP)) is associated with the N-terminal domains of these three proteins (55) preventing their activation. Unfolded proteins cause Grp78 to release PERK, IRE1 and ATF6 thus activating the UPR (33,55).

The now available luminal domains of PERK, ATF6 and IRE1 activate each of their specific signal cascades. Upon release from Grp78/Bip, PERK and IRE1 oligomerize in the ER membrane, causing PERK to autophosphorylate and activate its kinase activity. PERK, as previously mentioned, is an eIF2 kinase and similarly to GCN2 signals through eIF2 and the downstream proteins. PERK phosphorylation of eIF2 reduces general protein synthesis while promoting gene-specific translation of cellular mediators such as ATF4 (56) to aid in adaptation of ER stress. Similarly, IRE1 oligomerizes and autophosphorylates, activating endoribonuclease activity which splices X Box Binding Protein 1 (XBP1) (57), a transcription factor that increases expression of genes involved in restoring proteostasis. This precise excision of 26 nucleotides increases genes involved in ERAD, molecular chaperone synthesis and quality control (33,58). Upon the

movement of Bip/Grp78 from ATF6 to misfolded proteins, ATF6 translocates to the Golgi where it is cleaved and becomes active, yielding a transcription factor, which increases molecular chaperones as well as increasing XBP1 mRNA expression for IRE1 to process (33,59,60).

ER stress activation of the UPR is not just from the accumulation of misfolded proteins. The accumulation of unfolded proteins, misfolded proteins and altered ER $Ca^{+}$ signaling all activate the ER stress pathway. Additionally, changes in redox state within the lumen of the ER and disruption of the oxidative environment can alter the formation of disulfide bonds (61) and thus activate the ER stress pathway. Dysregulation of glucose sensing caused by prolonged periods of elevated sugar intake and hyperglycemia, can lead to ER stress which ultimately disrupts insulin secretion (62).

**PERK**

Pancreatic protein synthesis is necessary to maintain homeostasis within this critical organ. The exocrine portion of this tissue is responsible for the synthesis of about 20 key digestive enzymes (31) while the endocrine portion is responsible for insulin and glucagon synthesis. Similar to GCN2 evolving to handle the stress during amino acid deprivation, the UPR evolved to handle another important stress. PERK, one of the three components of the UPR serves to maintain functional levels of protein synthesis by monitoring and ensuring that production of newly synthesized proteins do not overload the ER. In the absence of this control system, the ER cannot adapt to the stress of the accumulated misfolded proteins and the system will be driven towards apoptosis (63). The

high protein turnover observed in the pancreas, due to its function as both an endocrine and exocrine gland make it subject to disregulation of ER homeostasis and proteostasis during times of stress.

PERK is abundantly expressed in the pancreas. This kinase is located in exocrine acinar cells (63), specifically in the basolateral portion of these cells where ER localizes (64) as well as endocrine beta cells in islets of Langerhans(63). Beta cells secrete insulin in large quantities to maintain blood glucose and thus have an abundance of highly developed ER.

Data shows that ER stress contributes to beta cell death in the pancreas (33) and that Type 2 Diabetes (T2D) is an example of ER stress causing disease (65). PERK deficient mice suffered beta cell death and developed diabetes. Prolonged PERK stimulation can lead to UPR induced beta cell death. PERK signaling through eIF2 preferentially translates ATF4 mRNA, which induces pro-apoptotic genes like CHOP. CHOP expression has been implicated as contributing to beta cell death (61,65–67) Furthermore, Oyadomari et al showed that in the Akita mouse which carries a mutation in the Insulin 2 gene and thus suffers from hyperglycemia and reduced beta cell mass. His studies showed that CHOP gene disruption prevented the ER stress mediated apoptosis of the beta cells (68). Additionally, Wolcott-Rallison Syndrome (WRS) is an autosomal recessive disease caused by mutations in the gene EIFAK3 which encodes for PERK protein(50). Onset of this disease occurs very early in life and patients experience pancreatic insufficiency due to cellular atrophy and endocrine and exocrine dysfunction.

**Gaps in Current Knowledge:**

The AAR pathway is essential for adaptation to the amino acid depletion induced by asparaginase (17). Previous data show there is a profound reduction in the ability of mice lacking GCN2 to adapt to amino acid stress (1,5,48,49)resulting in many negative phenotypes including hepatic steatosis, and increased mortality (27,69–71). Data also report that GCN2 is an important modulator of hepatic responses to asparaginase (48) however the involvement of this kinase as a protective agent within the pancreas is unknown. Prior studies which have examined the molecular mechanism of asparaginase toxicity have focused primarily on liver dysfunction. In addition to studying the liver, our laboratory has previously reported that loss of GCN2 in the thymus and spleen enhanced the immunosuppressive activity associated with asparaginase treatment (72) further showing the importance of this kinase in modulating the amino acid stress that occurs with asparaginase treatment. However, another major source of toxicity is pancreatitis, which results in termination of chemotherapy and results in cancer progression. Current literature focuses on how to help patients prevent or recover from AAP, however it remains unclear the mechanism of cellular disruption that leads to AAP. Thus we were interested in understanding the involvement of GCN2 in asparaginase - induced pancreatitis.

Previously, our laboratory has examined the effects of asparaginase on the pancreas following a single injection. While this provides insight in the acute ability of the pancreas to handle amino acid stress, it does not show how this

tissue is affected by prolonged amino acid starvation. Thus, the current study served to investigate a more clinically relevant treatment regimen, where circulating levels of asparaginase were maintained.

A major mechanism of hepatotoxicity has been elucidated, however there are many unanswered questions regarding the mechanism of asparaginase-associated pancreatitis. The studies performed in this thesis explore the role of GCN2 in modulating the effects of asparaginase treatment in the pancreas.

# MATERIALS AND METHODS

**Asparaginase preparation and activity**

*E.coli* derived asparaginase activity (Elspar; Merck, New Jersey, USA) was determined via Nesslerization technique to detect the level of ammonia as previously described (15,48,72). Using known ammonia standards, the production of ammonia by L-asparaginase over time was expressed relative to these known standards. The activity of the enzyme is expressed as international units (IU) where one IU is equivalent to the amount of L-asparaginase that catalyzed 1umol of ammonia per minute.

**Animals and experimental design**

All animal protocols were approved by the Institutional Animal Care and Use Committees (IACUC) at Rutgers, The State University of New Jersey. Animals studied were 8 week old male and female $GCN2^{+/+}$ (wildtype) and $GCN2^{-/-}$ mice backcrossed onto the C57BL/6J genetic background for 10 generations (Jackson Laboratories, Bar Harbor, ME). Male and female $GCN2^{-/-}$ mice of mixed genetic background (C57BL/6J and 129SvEv) were also studied. Animals were randomly assigned to receive either 8 daily intraperitoneal (IP) injections of native *E.coli* L-asparaginase in phosphate buffered saline (PBS) at 0 (control) or 3.0 (experimental) international units per gram of body weight (IU/g BW). Treatment groups were defined as follows: WP, $GCN2^{+/+}$ + PBS; WA, $GCN2^{+/+}$ + asparaginase; GP, $GCN2^{-/-}$ + PBS and GA, $GCN2^{-/-}$ + asparaginase. All treatment groups were gender balanced between males and females. Treatment groups received injections at the same time each day. 7.5 hours

following the 8th injection of treatment, mice were euthanized. Body weight was recorded each day throughout the study, as well as on the day of euthanasia.

Mice were fed commercial rodent chow (5001 Laboratory Rodent Diet, LabDiet). Cohorts of pure and mixed genetic background mice were freely fed and food intake was not assessed unless otherwise stated. In order to account for any differences that food intake may have caused, a pair-fed cohort was later established. Mice in these studies are referred to as pair fed. Food intake was measured daily for these animals and was pair fed to GCN2$^{-/-}$ treated with ASNase since it was observed that this treatment group consumed the least amount of food. GA mice were freely fed and each day food and spillage was weighed and calculated. The average food consumed was established for each day of injections and this weight plus average daily spillage was fed to mice in the other treatment groups. All mice in the pair fed cohort were of pure genetic background.

Mice were euthanized via decapitation and serum was collected from the trunk blood of the animal. Tissues were rapidly dissected, rinsed in PBS and weighed. The tissues were collected immediately; half of the pancreas was processed immediately for RNA isolation, while the other half was quickly frozen in liquid nitrogen to prevent tissue decay (27,48,49).

**Biomarkers of pancreatitis**

Serum amylase concentration was measuring using mouse serum from all four treatment groups by ELISA using the Amylase Activity Assay Kit (Sigma-Aldrich, St. Louis, MO)

**Pancreatic triglyceride concentration**

Triglycerides were measured from frozen prepared (see below) pancreas tissue lysates (~20 mg) using the Biovision Colorimetric Triglyceride Quantification Kit (Mountain View, CA) as per the manufacturer's instructions (49). The kit converts triglycerides within the tissue, to free fatty acids and glycerol. The converted glycerol is oxidized to generate a product that reacts with a kit specific probe to generate both a detectable color and fluorescence which is then measured.

**Immunoblot analysis**

Frozen pancreas tissue was weighed (~20 mg) and transferred to microcentrifuge tubes on ice in order to prepare protein lysates. Tissue was homogenized with eIF4E homogenization buffer containing 20 mM HEPES (pH 7.4), 2 mM EGTA, 50 mM NaF, 100 mM KCl, 0.2 mM disodium salt EDTA, 50 mM Beta-glycerophosphate, 1 mM DTT and 100 µl of PMSF in a 10 µl per 1 mg ratio. Homogenized tissue was then centrifuged at 10,000 x *g* for 10 min at 4° C. The supernatant was collected and combined 1:1 with SDS-page sample buffer. For specific antibody information refer to table 1.

**Table 1:** List of antibody's source, catalogue number, dilution, percentage gel and incubation time.

| **Antibody list** | **Source** | **Company** | **Catalogue #** | **Dilution** | **%Gel** | **Incubation** |
|---|---|---|---|---|---|---|
| p-eIF2 (Ser 51) | Rabbit | Cell Signaling Technolgies | 3597L | 1:5000 | 12.5 | Overnight |
| t-eIF2 | Rabbit | Life Technologies | 64-728P | 1:5000 | 12.5 | Overnight |
| p70 S6K1 total | Rabbit | Bethyl Laboratories | A300-510A | 1:2000 | 8 | Overnight |
| p-p70 S6K1 (Thr 389) | Rabbit | Cell Signaling Technolgies | 9205S | 1:5000 | 8 | Overnight |
| 4EBP1 | Rabbit | Bethyl Laboratories | A300-501A | 1:2000 | 15 | Overnight |
| p-AKT (Thr 308) | Rabbit | Cell Signaling Technolgies | 9275S | 1:2000 | 8 | Overnight |
| t-AKT | Rabbit | Cell Signaling Technolgies | 9272S | 1:5000 | 8 | Overnight |
| p-ERK1/2 (Thr202/Tyr204) | Rabbit | Cell Signaling Technolgies | 9101S | 1;1000 | 8 | Overnight |
| t-ERK1,2 | Rabbit | Santa Cruz Technologies | sc-93 | 1:2000 | 8 | Overnight |
| p-mTOR (Ser 2448) | Rabbit | Cell Signaling Technolgies | 2971S | 1:5000 | 8 | Overnight |
| t-mTOR | Rabbit | Cell Signaling Technolgies | 2972S | 1:5000 | 8 | Overnight |
| p-PERK (Thr 980) | Rabbit | Cell Signaling Technolgies | 3179S | 1:1000 | 8 | Overnight |
| | | | | | | |
| **Secondary antibody** | **Source** | **Company** | **Catalogue #** | **Dilution (5% milk)** | | **Incubation** |
| Goat anti-rabbit-HRP | Goat | Cell Signaling Technolgies | 7074 | 1:25000 | | 1 hour |

Additional preparation was required to examine the phosphorylation of 4EBP1. Following centrifugation, 100µl of supernatant was boiled at 110° C for 5 minutes and then centrifuged at 10,000 x *g* for 30 minutes at 4° C. A separate homogenization method was used to examine the phosphorylation of PERK and ERK(1/2). Tissue was homogenized with RIPA buffer containing 50mM HEPES (pH 7.5), 1% SDS, 3 mM Benzamidine, 1 mM Sodium Orthovanidate, 50 mM β-glycerophosphate, 2 mM EDTA, 1 mM microcystein, 1 mM Halt Cocktail, 1 mM PMSF and 50 mM NaF. Homogenized tissue was combined with 1:1 SDS-page sample buffer, centrifuged at 10,000 x *g* for 3 minutes. Proteins were then separated by SDS-PAGE and then electrophoretically transferred to polyvinylidene difluoride (PVDF) membranes for immunoblot analysis. For specific information regarding percentage of gels used, refer to table 1. Membranes were blocked in 5% non-fat milk diluted in TBST containing 20 mM Tris (pH 7.6), 150 mM NaCl, 0.02% Tween-20, and then incubated with the

corresponding antibody. Measurements of phosphorylation states of specified proteins were determined as previously described (27,48,49). For detection of primary antibodies, peroxidase-conjugated goat anti-rabbit antibody (1:25,000) was used). For specific antibody concentration refer to table 1.

Blots were imaged using enhanced chemiluminescence (Amersham Biosciences). Levels of protein expression were determined using both a Carestream Gel Logic 6000 imager as well as Protein Simple Machine. Quantification of band density was determined using Carestream Molecular Imaging Software (version 5.0) (2,27,48,49).

**Quantitative real-time PCR**

Total RNA was extracted from fresh mouse pancreas tissue immediately following dissection using RNeasy Plus Mini Kit (Quiagen, Maryland, USA). Immediately upon dissection, pancreas was weighed (~20 mg) and combined with 600 µl of Buffer RLT Plus for homogenization. Lysates were centrifuged for 3 min at 10,000 x *g*. The homogenized lysate was transferred to a gDNA Eliminator spin column and centrifuged for 30 sec at 10,000 x *g*. Six hundred µl of 70% ethanol was added to the flow through from the column and mixed via pipetting and added to an RNeasy spin column and centrifuged for 15 sec at 10,000 x *g*. Flow through was discarded and 700 µl of Buffer RW1 was added to the column and centrifuged for 15 sec at 10,000 x *g*. Flow through was again discarded. Five hundred µl of Buffer RPE was added to the spin column and rested for 5 min before centrifuging for 2 min at 10,000 x *g*. Again, the flow through was discarded. The RNeasy spin column was placed into a new collection tube and

50 µl of RNase-free water was applied directly to the spin column membrane before centrifuging for 1 min at 10,000 x *g* to elute the RNA. Elution was repeated an additional time with 50 µl of RNase-free water. In order to prevent potential contaminants, 100 µl of LiCl was added directly to the 100 µl of eluted RNA. This was placed in the -20° C freezer for 24 h. After sitting overnight, the tubes were spun for 15 min at 10,000 x *g*. The supernatant was discarded and the pellet was rinsed twice with 70% ethanol and centrifuged for 15 min at 10,000 x *g*. After the second spin, the supernatant was discarded and the pellet was suspended in 50 µl of RNase-free water.

Purified RNA concentration was determined via nanodrop. Samples were diluted so that each contained 1 µg of purified RNA. RNA was converted to cDNA using reverse transcription reagents from High-Capacity cDNA Reverse Transcription Kit (Applied Biosystems, Foster City, CA, USA). Changes in gene expression were determined by quantitative PCR using Taqman reagents. mRNA levels were confirmed using TaqMan Gene Expression Master Mix as well as TaqMan Gene Expression Assays (Applied Biosystems) were used for indicated genes of interest (48,49).

Using the StepOnePlus Real-Time PCR System (Applied Biosystems), amplification as well as detection was determined (27). mRNA from individual samples were measured in triplicate and normalized against β-Actin RNA. Data was obtained by using the comparative Ct method (49). Data is expressed as fold change compared to the experimental control (WP treatment group).

**Histology**

Frozen tissues were sectioned (10 μm) using a cryostat, and then were stained with Oil Red O to visualize lipid content in the pancreas as previously described (48,49). Pancreas tissue fixed in 4% paraformaldehyde was sent to the Rutgers University Histopathology Lab for sectioning and staining with hematoxylin and eosin to characterize histological differences under light-microscopy.

Frozen tissues were sectioned (10 μm) using a cryostat, and then were treated with TUNEL Apoptosis Detection Kit (For Cryopreserved Tissue Section, FITC labeled POD) (GenScript, New Jersey, USA) according to manufacture's protocol.

Fresh tissue was fixed for electron microscopy in a solution of 4% paraformaldehyde, 2.5% glutaraldehyde and 1 x PBS for 2-4 hours. Tissue was rinsed 3 x 10 minutes in 1 x PBS. Tissue remained in 1 x PBS at 4°C until it was sent to the laboratory of Dr. Geoffery McAuliffe for routine preparation for transmission electron microscopy.

**Serum amino acids**

Serum was obtained by centrifugation of trunk blood collected as described above. Samples were analyzed via HPLC using ortho-phthalaldehyde/9-fluorenylmethyl chloroformate (OPA/FMOC) derivatized amino acid analysis. Detection was performed according to Agilent protocol app note: 5990-4547EN using Agilent ZORBAX Eclipse Plus C18 column. Derivatization reagents used including Borate Buffers, OPA and FMOC were ready-made

solutions purchased from Agilent. HPLC column was equilibrated using two mobile phases, Mobile phase A (10 mM $Na_2HPO_4$, 10 mM $Na_2B_4O_7$, 5 mM $NaN_3$ pH 8.2), Mobile phase B (acetonitrile, methanol and water) and run for 30-60 minutes. A pre-column derivatization/injection procedure of 1 vial borate butter, 1 vials OPA, 1 vial FMOC, 1 vial injection diluent, 1 vial blank followed by samples respectively was established as a sequence template. Prior to running samples, amino acid standards were prepared as described within the Agilent protocol.

Serum amino acid preparation: 180 µl of 0.1% formic acid in methanol was aliquotted into Eppendorf tubes. Sixty µl of serum was added and immediately vortexed. The solution was added to Captiva Non-Drip Lipids Filtration 3mL columns. After sitting for 5 minutes in the columns, the solution was filtered using a 3CC syringe plunger and the eluent was collected in an additional Eppendorf tube. Twenty µl of eluent was aliquotted into an insert vial along with 5 µl of an internal standard (sarcosine and norvaline), placed into an autosampler vial and vortexed. A calibration curve using five point calibrations of early, middle and late eluting amino acids, was established using the provided amino acid standards in order to calculate $R^2$ values. Using these calibration curves, serum concentration of amino acids (pmol/µl) was determined using Agilent 1200 Series SL.

**Liver protein synthesis**

Liver protein synthesis was determined by using the flooding dose technique. In order to determine tissue protein synthesis, fifteen minutes prior to decapitation, mice were intraperitoneally injected with 250 mg of DL-[$^2H_5$]phenylalanine per kg of body weight. Use of phenylalanine is preferable to

the use of leucine since phenylalanine is more soluble than leucine and the pool of free phenylalanine is smaller within tissue than the pool of free leucine (73). Individual tissue samples were processed as previously described (69) to assess enrichment of labeled phenylalanine incorporation into liver protein. Approximately 50 mg of frozen powdered tissue was weighed and 1 mL of cold 3% Perchloric Acid (PCA) was added. Samples were vortexed and sat on ice for 10 minutes. Following this brief incubation, samples were centrifuged at 8,000 x *g* at 4°C for 5 min. The supernatant was collected and was used as the Intracellular Amino Acid Enrichment which was stored at -20°C until further processing. The pellet was washed twice with 1.75 mL of cold 3% PCA was added to re-suspend the pellet, which was then centrifuged at 8,000 x *g* at 4°C for 5 min. Then, 1.35 mL of deionized water was added to the pellet followed by 150 µl of 3M NaOH. Samples were then heated for 1 h at 37°C with intermittent vortexing every 15 min. After heating, 300 µl of 40% PCA was added to the samples, which then were put on ice for 15 min. Samples were centrifuged at 8,000 x *g* at 4°C for 5 min and the supernatant was discarded. The pellet was washed 3 times with 1.75 mL of 3% PCA and centrifuged at 8,000 x *g* at 4°C for 5 min with each wash. Following the third wash, pellets were either stored in the refrigerator at 4°C or were taken through the hydrolysis process.

The aforementioned pellets were re-suspended with 1 mL of 6N HCl and transferred to locking eppendorf tubes. Samples were hydrolyzed for 24 h at 110°C with intermittent vortexing every 6-8 hours. One hundred and fifty µl of hydrolyzed sample was used for derivitization. To eliminate large particles,

samples were centrifuged at 8,000 x *g* for 10 minutes. One hundred µl of supernatant was added to autosampler vials and dried by savant (Savant Speed Vac Kit; Fisher Scienfic, MA). Upon drying completing, 100 µl of acidic isobutanol was added and samples were heated for 1 hr at 85°C. Samples were again dried in the savant. Samples were reconstituted in 75 µl of 20% acetonitrile on morning of processing through the LCMS.

The intracellular cellular amino acid portion of each sample was purified through ion exchange column using AG 50W-X8 Resin (Bio-Rad, California). 1mL of intracellular sample was added to the column. Column flow through was collected by running 1M $NH_4OH$ through the column. Samples were dried overnight by savant and derivatized as described above.

Determination of isotopic enrichment was measuring using the ions mass to charge ratio (m/z) 336 and 341 of the tertiary butyldimethylsilyl derivative. Liver protein fractional synthesis rate (FSR) was calculated from the enrichment of phenylalanine incorporated into tissue.

**Data analysis and statistics**

Results were analyzed using STATISTICA, statistical software package (StatSoft, Tulsa, OK). Data is reported as means ± SEM. Differences between treatment groups were analyzed by two-way ANOVA, with mouse strain and drug as the independent variables. When an overall significance was detected, differences among individual means were evaluated using Tukey's post-hoc test. A significance of $P<0.05$ was utilized for all statistical analysis.

# RESULTS

## Body Composition

In vivo effects of asparaginase treatment on body composition were determined in three different cohorts of mice. Freely fed pure genetic background (C57BL6J), mixed genetic background (C57BL/6J and 129SvEv) and pair-fed pure genetic background mice were monitored for body weight changes by weighing the animals prior to treatment and on the final day of injection. The freely fed GCN2$^{-/-}$ mice with a pure genetic background treated with asparaginase showed the greatest overall decrease in body weight, which was significant compared to the other treatment groups (Fig 7A). Similarly in the freely fed mixed genetic background mice cohort, the GCN2$^{-/-}$ mice treated with asparaginase exhibited significantly decreased overall body weight (Fig 7B). The mice in the pair fed cohort all showed a decrease in body weight, however both groups treated with asparaginase (WA, GA) showed greater weight loss than the groups treated with PBS (Fig 7C). These results support a negative effect of asparaginase on body weight independent of energy intake.

A recognized feature of pancreatitis is an increase in pancreas mass (74). The wet weight of the pancreas at the time of euthanasia was determined in both cohorts of freely fed mice as well as the pair fed mice cohort. In both freely fed and pair fed cohorts, GA mice exhibited significantly larger pancreas weights than other treatment groups (Fig 8A, 8B). In the mixed genetic background mice, both WA and GA mice exhibited larger pancreas weights than mice treated with

PBS (P=0.05)(Fig 8C). These results support that treatment with asparaginase leads to larger pancreas weights in $GCN2^{-/-}$ mice than in animals with intact GCN2 implicating the GCN2 pathway as relevant to this process.

Pancreas weight expressed as a percentage of body weight was studied in freely fed animals with a pure or mixed genetic background, as well as in pair fed mice by examining the wet weight of the pancreas at the time of sacrifice as a percentage of total body weight. Both GA groups from the freely-fed and pair fed cohorts exhibited larger pancreas as a percentage of body weight than any other treatment group (P=0.05) (Fig 9A, 9C) while the GP groups from both pure genetic freely-fed and pair-fed cohorts exhibited larger pancreas relative to body size than either of the $GCN2^{+/+}$ treatment groups. Mixed genetic background mice treated with asparaginase had the highest pancreas weight as a percentage of their body weight regardless of the presence of absence of GCN2 (Fig 9B).

**Serum Amino Acid Analysis**

Circulating concentrations of amino acids were measured 8 hours after the eighth and final injection of asparaginase. Serum levels of aspartic acid (asp), glutamic acid (glu), asparagine (asn) and glutamine (gln) were determined by HPLC. Treatment with asparaginase significantly decreased circulating levels of both asparagine as well as glutamine regardless of genetic background (Supplemental Figure 1).

**Histological Differences**

Hematoxylin and eosin staining revealed visual differences between pancreata of WT and GCN2$^{-/-}$ mice (Fig 10A). Regardless of treatment, GCN2$^{-/-}$ pancreas exhibited tighter cellular boundaries and more intercellular space than pancreas from WT mice. H&E staining of the GA group showed increased acinar cell size compared to other treatment groups as well as altered staining of zymogen granules. Electron microscopy of GA pancreas revealed highly disrupted ER (Supplemental Fig 2) in addition to a distorted nuclear envelope, features not seen in pancreas of WT mice.

To address the mechanism of pancreatitis induced by asparaginase, and the degree of insult to the pancreas in the absence of GCN2, a TUNEL assay was performed in order to follow levels of DNA fragmentation as a result of cell apoptosis. Interestingly, TUNEL-positive cells were detectable in all samples and no significant differences were observed among the treatment groups (Fig 10B). We speculate this may be due in part to the high degradative nature of pancreas tissue following dissection (75). Additionally, for this assay, we sectioned unfixed frozen pancreas tissue, which may have allowed for additional degradation to occur.

**Lipid Accumulation**

Whole body deletion of GCN2 reportedly promotes hepatic lipid accumulation during treatment with asparaginase (49). In order to determine if the increase in pancreas mass was due to an accumulation of lipid within the pancreas, Oil Red O staining was used to visualize neutral lipid content within the tissue. Biochemical analysis of pancreatic triglyceride content was used to

corroborate or clarify differences in Oil Red O staining. In contrast to previously published data in liver, GA mice exhibited significantly lower concentrations of triglycerides then GP mice (Fig 10C). Concentration of triglyceride in GP livers was significantly higher than both WP and WA (Fig 10D). These results indicate that the increase in pancreas mass following asparaginase treatment is not due to the accumulation of lipid.

**AAR Pathway Activation**

Deprivation of a single amino acid activates GCN2. Activated GCN2 will phosphorylate the α-subunit of eIF2. Phosphorylation of eIF2 decreases global protein synthesis while simultaneously increases translation of specific mRNAs to aid in cellular adaptation. One of the essential genes for this adaptation is translation of ATF4 and its induction of ASNS. Inability of the cell to adapt to amino acid stress results in cell death through apoptosis (15,25,27). In our studies, phosphorylation of eIF2 in the pancreas did not differ across treatment groups (Fig 11A).

Certain genes that were examined showed a lot of variance only in the GA group the way data was originally displayed (Fig 11C). We decided to examine the individual the pancreas of specific animals to see if any physical differences were present that could account for this discrepancy. When the weight of the pancreas was expressed as a percentage of body weight of each individual animal, the animals that had lower pancreas weights were the same animals that expressed lower mRNA levels. Conversely, the animals that had the largest pancreas relative to body weight were the animals that expressed higher levels

of mRNA. We determined that it was appropriate to additionally express mRNA levels for this treatment group as a bimodal distribution; comparing animals that have started to activate the stress response and thus had larger pancreas mass when expressed relative to body size vs animals that have not suffered as much cellular stress that had lower pancreas mass when expressed relative to body size. Quantitative RT-PCR indicates downstream transcription factor ATF4 and ASNS were preferably transcribed in GA pancreas when data was expressed as a bimodal distribution (Fig 11D).

ERK(1/2) is part of the MAP kinase signaling pathway and is involved in a wide variety of processes including primarily cell cycle processes as well as cell survival (76). In this study, western blot analysis showed no significant differences were induced between treatment groups on ERK(1/2) phosphorylation (Fig 11B) suggesting little involvement of the MAP kinase pathway in the cellular responses during asparaginase treatment. Alternatively, the heterogeneity of the tissue could have masked cell-specific effects in this signaling event.

Published studies suggest that FGF21 expression within the pancreas may serve a protective function. Immediately following pancreatic injury, FGF21 is rapidly expressed (77). FGF21 mRNA expression was measured by qRT-PCR to determine the presence of this protective hormonal regulator. FGF21 was highly expressed in the pancreas from GA mice demonstrating the greatest tissue enlargement but then absent in expression in other mice, resulting in high variance in the GA group (Fig 11E). The high levels of FGF21 expression in

some GA samples suggests the stress associated with asparaginase was damaging in the pancreas of these mice. In this study, there was no correlation between FGF21 expression and EGR1 expression.

CHOP, also known as DNA damage-inducible transcript 3, is a member of the bZIP transcription factor family and is heavily involved in cell cycle and apoptotic pathways (34,78). Although downstream of ATF4, CHOP mRNA expression did not differ between treatment groups (9C). An additional eIF2 kinase, PERK, previously named pancreatic eIF2 kinase, is more highly expressed within the pancreas and thus may be responsible for the equal phosphorylation of eIF2 across treatment groups and may also be responsible for gene expression of downstream targets of eIF2 phosphorylation.

**Activation of ER Stress Pathway**

Accumulation of misfolded proteins within the ER has been shown to activate branches of the ER stress pathway, also referred to as the unfolded protein response (UPR). This can activate an additional eIF2 kinase, PERK that works in conjunction with IRE1 and ATF6 to respond to this type of cellular stress. The three sensors of ER stress, PERK, IRE1 and ATF6 are negatively regulated by BiP/Grp78, which interacts with each of these under non-stressed conditions (79). X-box binding protein 1 (XBP1) is a transcription factor that following removal of introns by IRE1 becomes active and upregulates other genes involved in the adaptation to ER stress. Under ER stress conditions Spliced XBP1 and ATF6 work together to modulate transcription of specific chaperone proteins (78). Phosphorylation of PERK within the pancreas was

significantly upregulated within the pancreas of GCN2$^{-/-}$ mice (Fig 12A) suggesting activation of the UPR. CHOP plays an integral role as a transcription factor in both the AAR and ER stress pathways. Similar to CHOP is another member of bZIP transcription factor family, C/EBPβ, CCAAT/enhancer binding protein β which is involved in inflammatory pathways and regulation of macrophages (25,34,80). Like CHOP, there were no differences in gene expression observed between treatment groups for C/EBPβ (Fig 12B). These studies showed that both ATF6 and BiP/Grp78 mRNA levels were highly expressed in stressed GA mice supporting that asparaginase activates the ER stress pathway in the absence of GCN2 (Fig 12C). Interestingly, XBP1 splicing was found to be highest in GCN2$^{-/-}$ animals in both control and drug treatment groups (Fig 12B), suggesting that the absence of GCN2 causes elevation of ER stress from baseline. EGR-1 regulates ATF3, expression which is related to cellular damage and cell death (81). Expression of ATF3 appeared to be lower in GCN2$^{-/-}$ mice than wildtype animals, and was also significantly elevated in the stressed GA mice (Fig 12C). The expression of these genes suggests full activation of the ER stress pathway within GCN2 null mice.

**Biomarkers of Pancreatitis**

We next examined the expression of several possible biomarkers associated with pancreatitis. Amylase is an enzyme produced in the pancreas. Measurement of serum amylase is a commonly used biomarker of pancreatic injury. Therefore we examined mouse serum from wildtype animals vs GCN2$^{-/-}$ animals treated with either control (saline) or asparaginase. Amylase activity as

determined by ELISA (Sigma-Aldrich) did not differ between treatment groups (Fig 13A).

Similarly, Pancreatitis Associated Protein, PAP, is a protein that is expressed under pathological conditions and can be useful for the diagnosis of acute pancreatitis (82). Similar to markers of ER stress, only some GA mice displayed increases in PAP mRNA expression with the remaining showing no expression, suggesting heterogeneity in the timing of tissue dysfunction (Fig 13B) (Fig 13C).

Tumor necrosis factor alpha (TNF$\alpha$) is a signaling factor involved in systemic inflammation as well as implicated in a host of autoimmune and inflammatory conditions (83). We observed that, TNFα was elevated in only when displayed in bimodal distribution (Fig 13C).

SIRT1 is a member of the sirtuin family and can modulate a variety of cellular functions including DNA damage, apoptosis and autophagy (35). As expected, SIRT1 gene expression levels were highest in stressed GA mice (Fig 13C). Another important marker, Early Growth Response 1 (EGR-1) is a zinc finger transcription factor which acts to regulate proinflammatory genes (84,85). EGR-1 expression is involved with promoting pathogenesis of acute pancreatitis (85) and its expression may be blunted by FGF21 signaling (77). EGR-1 mRNA expression as measured by qRT-PCR was performed in order to determine the presence of this pro-inflammatory transcription factor. Interestingly, there were no significant increases in expression of EGR-1 among treatment groups; instead EGR-1 expression was lowest in the GA group (Fig 13B). Although serum

amylase levels were not significantly increased, the presence of multiple inflammatory markers as well as both hepatic and pancreatic PAP mRNA expression supports that there is significant induction of tissue dysfunction following treatment with asparaginase. Due to the high variance between animals, there was no apparent difference when data was considered together.

**Protein Synthesis**

Amino acid deprivation results in a decrease of global protein synthesis and simultaneous up regulation of genes involved in alleviating this stress (69). Reductions in amino acid supply are also detected by the mTORC1 signaling pathway. Previous data from our laboratory show that pancreatic phosphorylation of 4EBP1 and S6K1 are reduced following a single injection of *E.coli* asparaginase (15). Following 8 IP injections with asparaginase, phosphorylation of 4E-BP1 and S6K1 were not significantly different between treatment groups. However, there was less expression of total 4E-BP1 and S6K1 proteins in both WA and GA groups (Fig 14A and 14B). Similarly, phosphorylation of mTOR (Fig 14C) was lower in both WA and GA groups, while phosphorylation of Akt (Fig 14D) was highest in both of these treatment groups. In other words, in contrast with results following a single injection, no significant changes in mTORC1 signaling were noted in the pancreas after 8 IP injections with asparaginase.

**Evidence of Hepatic Stress**

Hepatotoxicity is one of the most common side effects during asparaginase treatment. Previously, our lab showed the impact of GCN2 in modulating liver adaptation during asparaginase treatment (15,27,48,49). In the

current study, hepatic PAP gene expression only occurs in stressed GA mice (Fig 15A).

Additionally, fractional synthesis rate of liver protein synthesis was determined by examining the incorporation of labeled phenylalanine via the flooding dose method (15). Treatment with asparaginase caused a decrease in FSR in both WA and GA treatment groups (Fig 15B). These results stand in contrast with data previously collected after a single injection in which general protein synthesis was significantly reduced only in wild type mice (15). Thus, other auxiliary adaptive responses must exist to reduce protein synthesis during longer treatment in $GCN2^{-/-}$ mice. This requires additional study to reconcile.

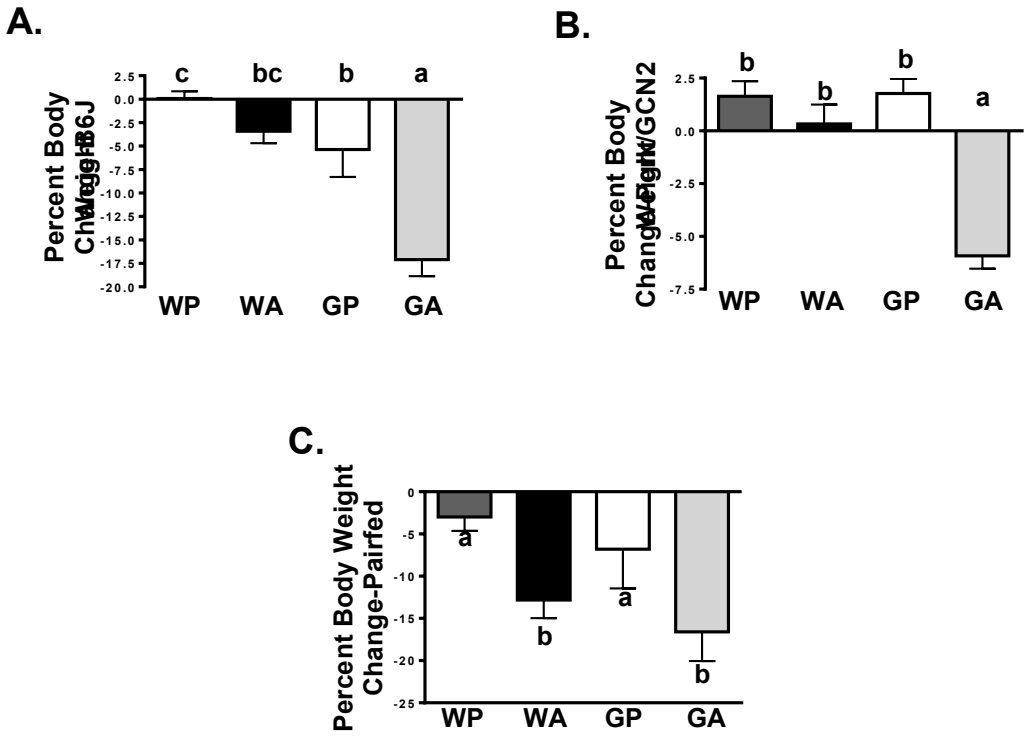


**Figure 7:** Asparaginase reduces body weight of ad libitum-fed and pair fed GA mice. **A:** Pure genetic background mice (n=8-23). Significant interactions between strain and treatment (P=0.05) **B:** Mixed genetic background (n=22-26 per group). Significant interactions between strain and treatment (P=0.001) **C:** Mice were pair fed to the GCN2KO treated with asparaginase (n=5-6 per group). Significant differences between treatments (P<0.005) Significant difference in strain and treatment (P<0.001 and P<0.05 respectively). Significant interactions between strain and treatment (P<0.05). All animals were 8 week old and received 8 IP injections. Labeled means without a common letter were significantly different (P=0.05). Values are means and error bars indicate SEM. X-axis represents treatment groups. WP, wild-type mice+PBS; WA, wild-type mice+asparaginase; GP, $Gcn2^{-/-}$mice+PBS; GA, $Gcn2^{-/-}$ mice+ asparaginase.

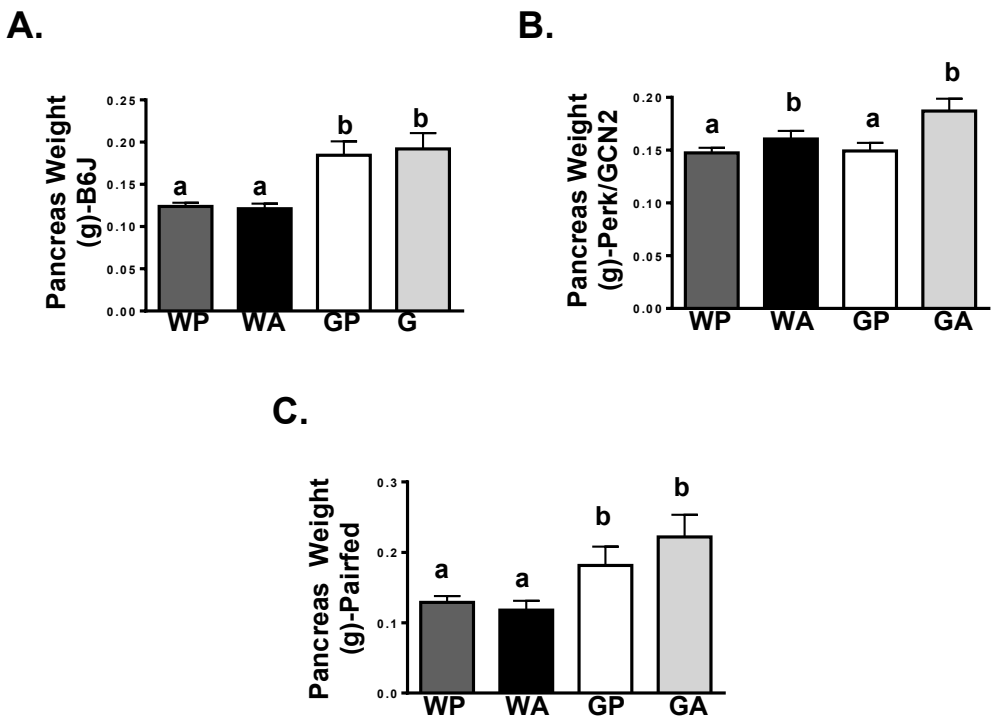


**Figure 8:** Pancreas wet weight was greatest in GCN2 null mice treated with asparaginase. **A:** pure genetic background (n=8-23 per group). Significant difference in strain ($P<0.005$) **B:** Mixed genetic background mice (n=22-26 per group). Significant difference in treatment ($P<0.005$) **C:** Pair fed to the GCN2 KO treated with asparaginase (n=5-6 per group). Significant differences between strains ($P=0.001$). Significant difference in strain and treatment ($P<0.001$ and $P<0.05$ respectively). Significant interactions between strain and treatment ($P<0.05$). All animals were 8 week old and received 8 IP injections. Labeled means without a common letter were significantly different ($P=0.05$). Values are means and error bars indicate SEM. X-axis represents treatment groups. WP, wild-type mice+PBS; WA, wild-type mice+asparaginase; GP, $Gcn2^{-/-}$mice+PBS; GA, $Gcn2^{-/-}$ mice+ asparaginase.

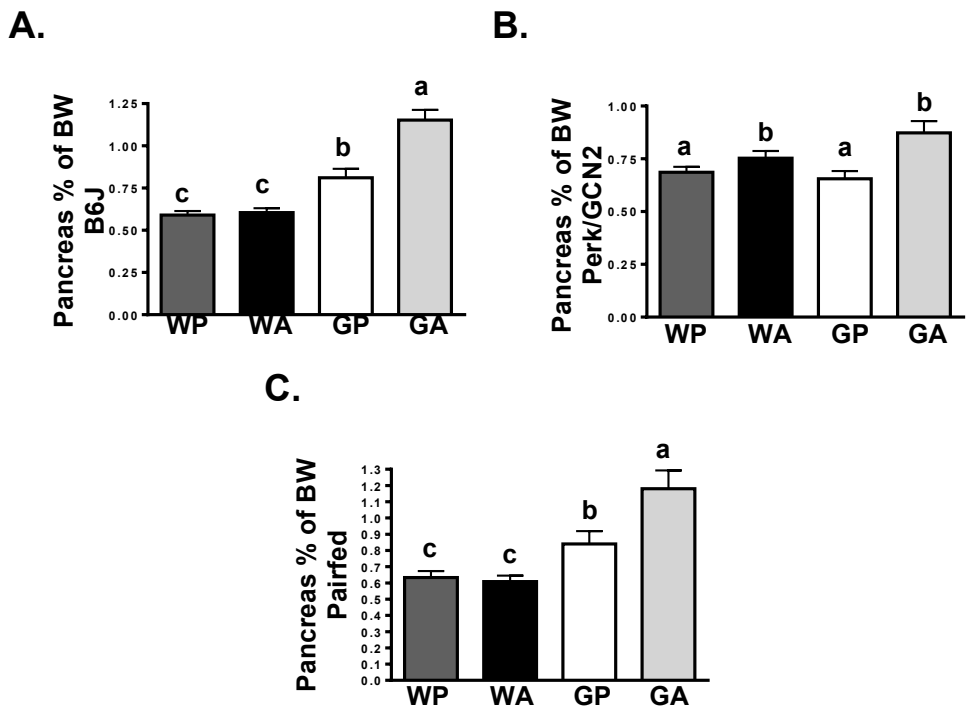


**Figure 9:** Pancreas weight expressed relative to body weight was greatest in GCN2 null mice treated with asparaginase. **A:** Pure genetic background mice (n=8-23 per group). Significant difference in strain and treatment ($P<0.001$) Significant interactions between strain and treatment ($P<0.05$) **B:** Mixed genetic background mice (n=22-26 per group). Significant difference in treatment ($P<0.001$) **C:** Mice were pair fed to the GCN2KO treated with asparaginase (n=5-6 per group). Significant difference in strain and treatment ($P<0.001$ and $P<0.05$ respectively). Significant interactions between strain and treatment ($P<0.05$). All animals were 8 week old and received 8 IP injections. Labeled means without a common letter were significantly different ($P=0.05$). Values are means and error bars indicate SEM. X-axis represents treatment groups. WP, wild-type mice+PBS; WA, wild-type mice+asparaginase; GP, $Gcn2^{-/-}$mice+PBS; GA, $Gcn2^{-/-}$ mice+ asparaginase.

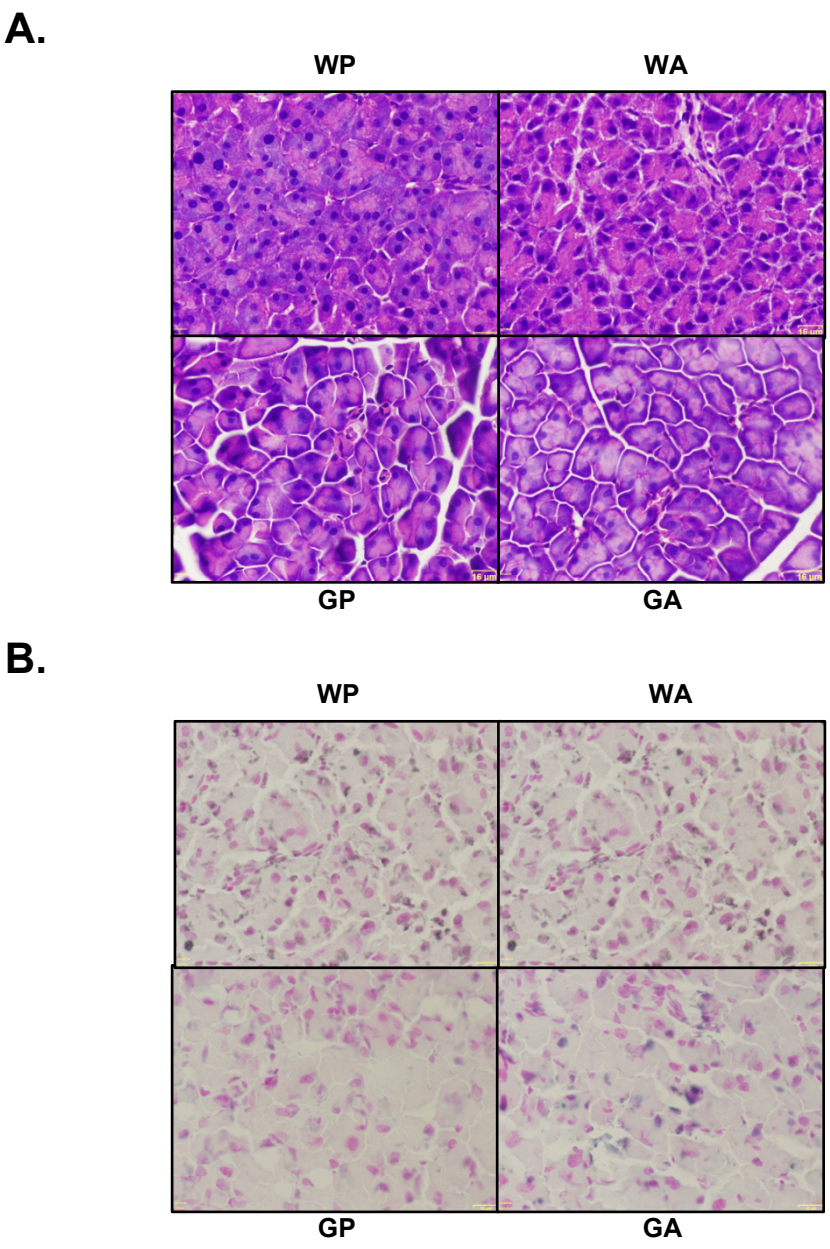


**Figure 10:** General Histology **A:** Hematoxylin & eosin staining showed increased acinar cell size and altered staining of zymogen granules in GA mice **B:** TUNEL staining showed little to no cell death in any treatment group.

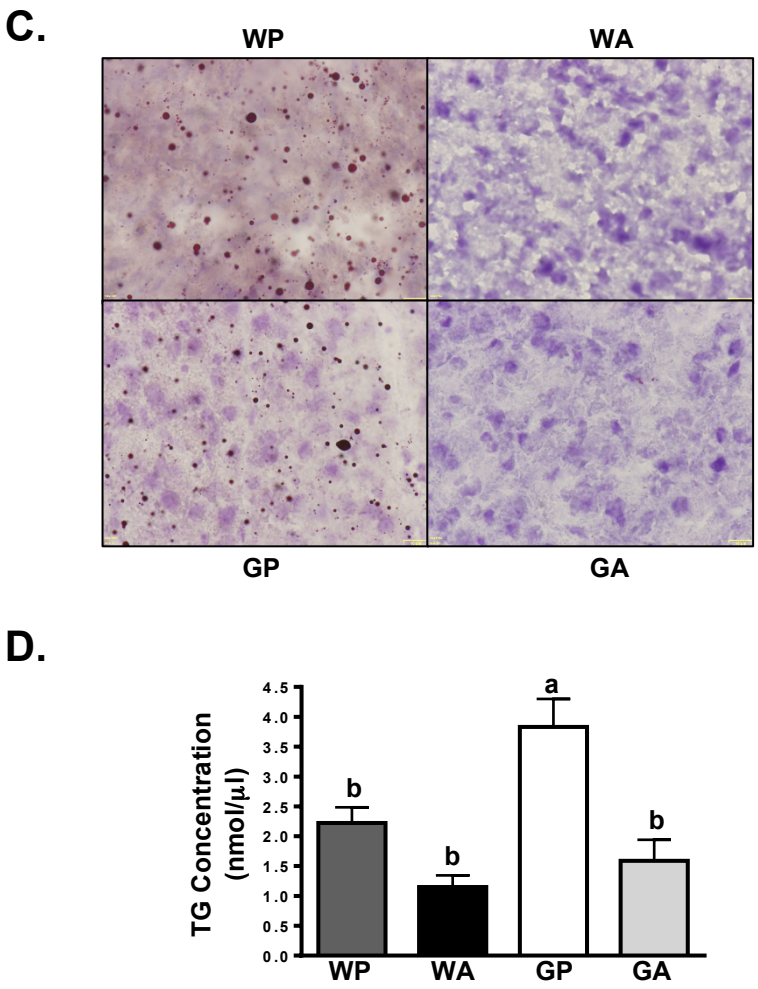


**Figure 10:** General Histology **C:** Oil Red O stain showed that asparaginase reduced lipid content in pancreas **D:** Triglyceride assay. Values are mean triglyceride concentration in nanomoles, per microliter. Error bars indicate SEM. X-axis represents treatment groups. Two way-ANOVA indicated that differences in both strain and treatment were significant ($P<0.005$ and $P<0.001$ respectively). Labeled means without a common letter were significantly different ($P<0.001$). WP, wild-type mice+PBS; WA, wild-type mice+asparaginase; GP, $Gcn2^{-/-}$mice+PBS; GA, $Gcn2^{-/-}$ mice+ asparaginase. All images taken at 16µM.

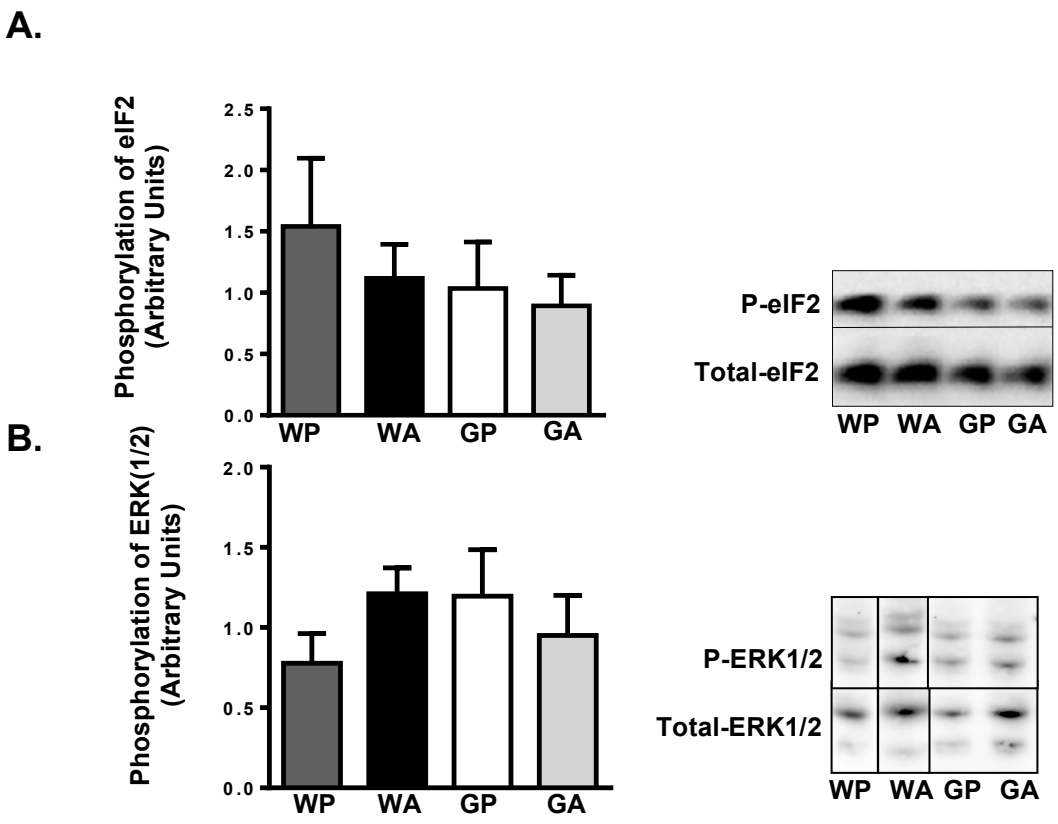


**Figure 11:** Activation of the amino acid response (AAR) pathway in pancreas via phosphorylation of eIF2 was not altered by asparaginase in the pancreas of wild type and GCN2 null mice. **A:** Phosphorylation of eukaryotic initiation factor 2 (eIF2) expressed as band density of serine 51 phosphorylation relative to total eIF2-α by immunoblot analysis. **B:** Phosphorylation of ERK(1/2) expressed as band density of serine 51 phosphorylation relative to total eIF2-α by immunoblot analysis Labeled means without a common letter were significantly different (P=0.001). All animals were 8 week old, B6J mice which received 8 IP injections of treatment. Mice were pair fed to the GCN2KO treated with asparaginase. Error bars indicate SEM. X-axis represents treatment groups. WP, wild-type mice treated with PBS; WA, wild-type mice treated with asparaginase; GP, Gcn2 null mice treated with PBS; GA, Gcn2 null mice treated with asparaginase.

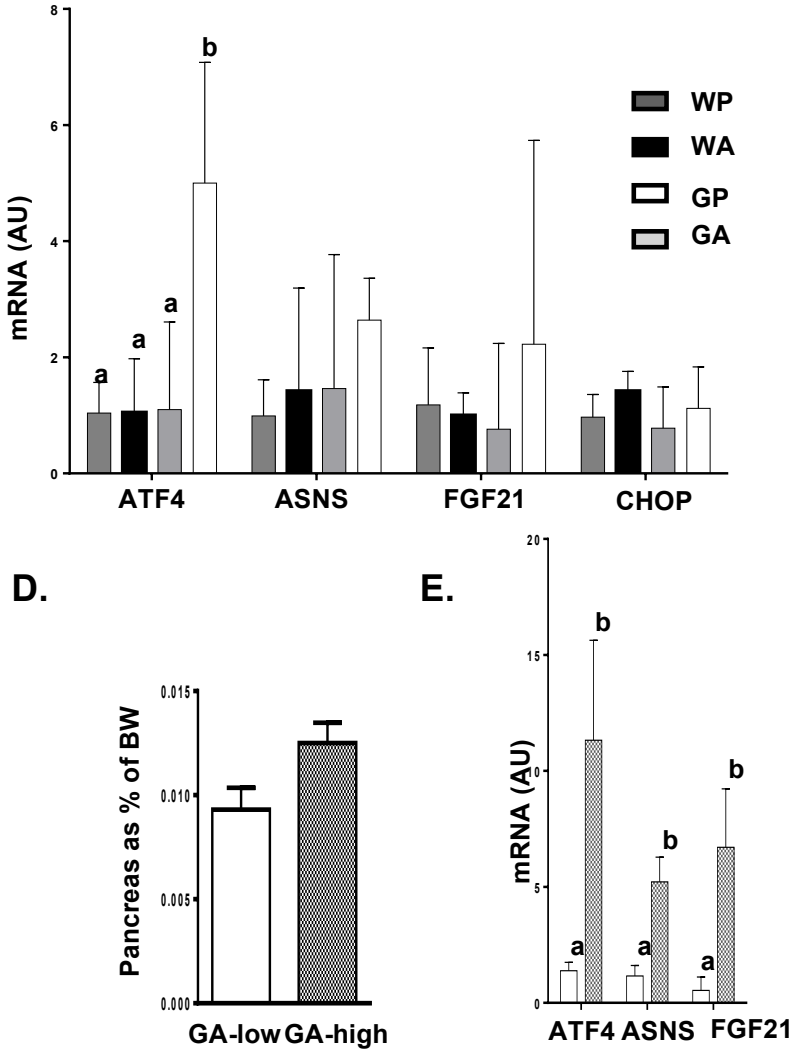


**Figure 11:** Activation of the AAR **C:** ATF4, ASNS, FGF-21 and CHOP mRNA expression as measure by qRT PCR (n=4-11 per group). **D:** Pancreas weights of animals used for gene expression data expressed as a percentage of body weight. **E:** Bimodal distribution of gene expression in GA pancreas. White=GA animals with lower pancreas weight not yet showing signs of distress, Pattern= GA animals with higher pancreas weights starting to show signs of distress. Labeled means without a common letter were significantly different (P=0.001). All animals were 8 week old, B6J mice which received 8 IP injections of treatment. Mice were pair fed to the GCN2KO treated with asparaginase. Error bars indicate SEM. X-axis represents treatment groups. WP, wild-type mice treated with PBS; WA, wild-type mice treated with asparaginase; GP, Gcn2 null mice treated with PBS; GA, Gcn2 null mice treated with asparaginase.

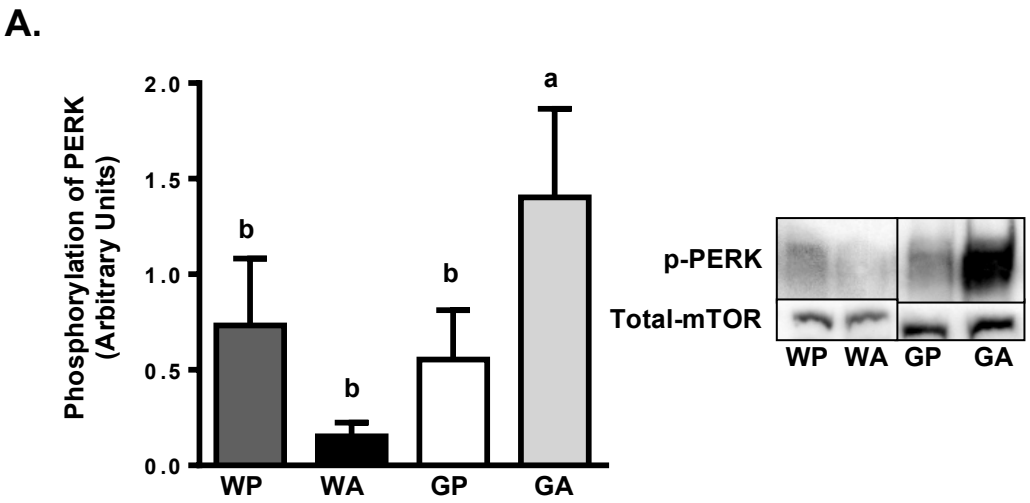


**Figure 12:** Asparaginase treatment causes ER stress and activates UPR in GA pancreas. **A:** Phosphorylation of PERK at the threonine 980 phosphorylation site, normalized for total mTOR measured by immunoblot analysis (n=6 per group)

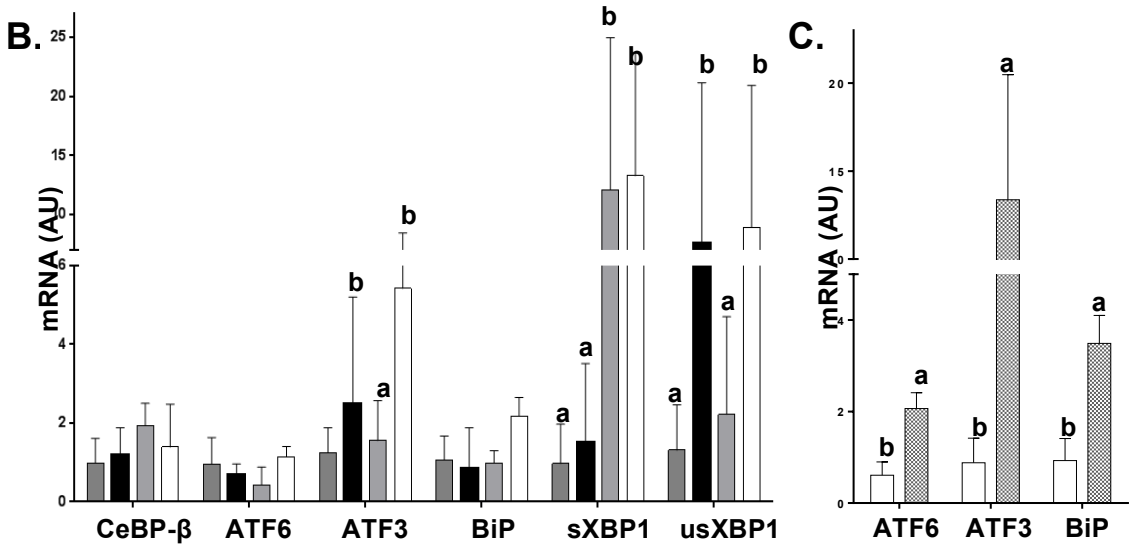


**Figure 12:** Asparaginase treatment causes ER stress and activates UPR in GA pancreas. **B:** C/EBP-β, ATF6, BiP, ATF3, xBP1 spliced and xBP1 unspliced mRNA expression as measured by quantitative real-time PCR (n=5-11 per group). **C:** Bimodal distribution of gene expression in GA pancreas. White=GA animals with lower pancreas weight not yet showing signs of distress, Pattern= GA animals with higher pancreas weights starting to show signs of distress. Labeled means without a common letter were significantly different (P=0.001). WP, wild-type mice treated with PBS; WA, wild-type mice treated with asparaginase; GP, Gcn2 null mice treated with PBS; GA, Gcn2 null mice treated with asparaginase

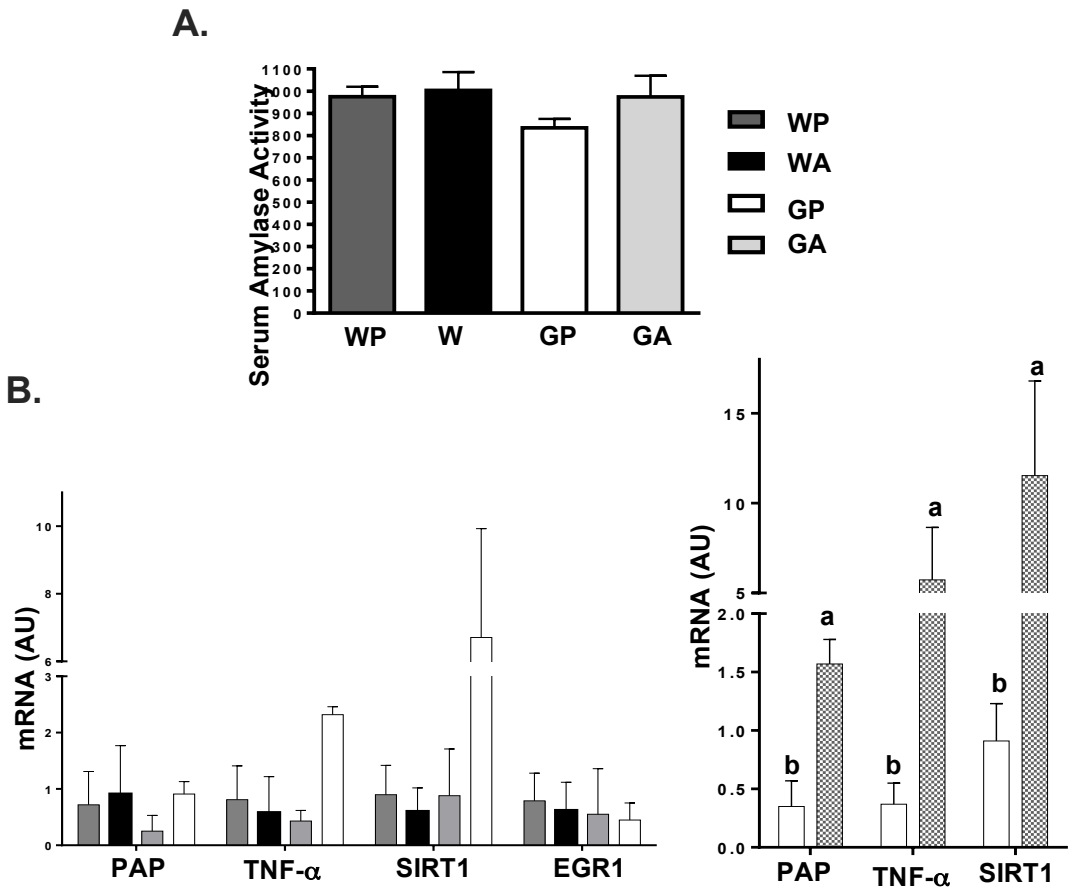


**Figure 13:** Biomarkers of Pancreatitis. **A:** Serum Amylase activity did not differ among treatment groups. Serum amylase activity following 8IP injections of treatment (n=8 per group). **B:** PAP, TNF-α , SIRT1 and EGR1 mRNA expression as measure by quantitative real-time PCR (n=4-11 per group). **C:** Bimodal distribution of gene expression in GA pancreas. White=GA animals with lower pancreas weight not yet showing signs of distress, Pattern= GA animals with higher pancreas weights starting to show signs of distress. Animals received 8IP injections of treatment. Mice were 8 weeks of age from mixed genetic background. Values are means and error bars indicate SEM. X-axis represents treatment groups). Labeled means without a common letter were significantly different (P=0.001). WP, wild-type mice+PBS; WA, wild-type mice+asparaginase; GP, $Gcn2^{-/-}$mice+PBS; GA, $Gcn2^{-/-}$ mice+ asparaginase.

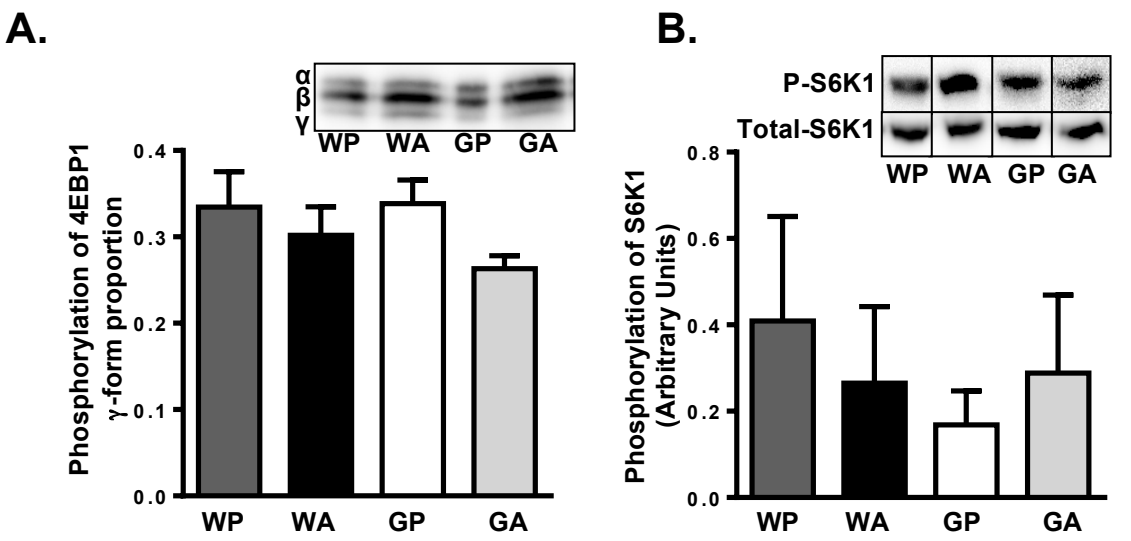


**Figure 14:** Treatment with asparaginase does not disrupt mTOR signaling pathway**. A:** Phosphorylation of 4EBP1 as determined by decrease in mobility measured by immunoblot analysis (n=6 per group). **B:** Phosphorylation of S6K1 at the threonine 389 phosphorylation site, normalized for total S6K1 measured by immunoblot analysis (n=6 per group). . Animals were 8 week old, pure genetic background mice which received 8 IP injections of treatment. Mice were pair fed to the GCN2KO treated with asparaginase Values are means and error bars indicate SEM. X-axis represents treatment groups. Labeled means without a common letter were significantly different (P=0.05). WP, wild-type mice treated with PBS; WA, wild-type mice treated with asparaginase; GP, Gcn2 null mice treated with PBS; GA, Gcn2 null mice treated with asparaginase.

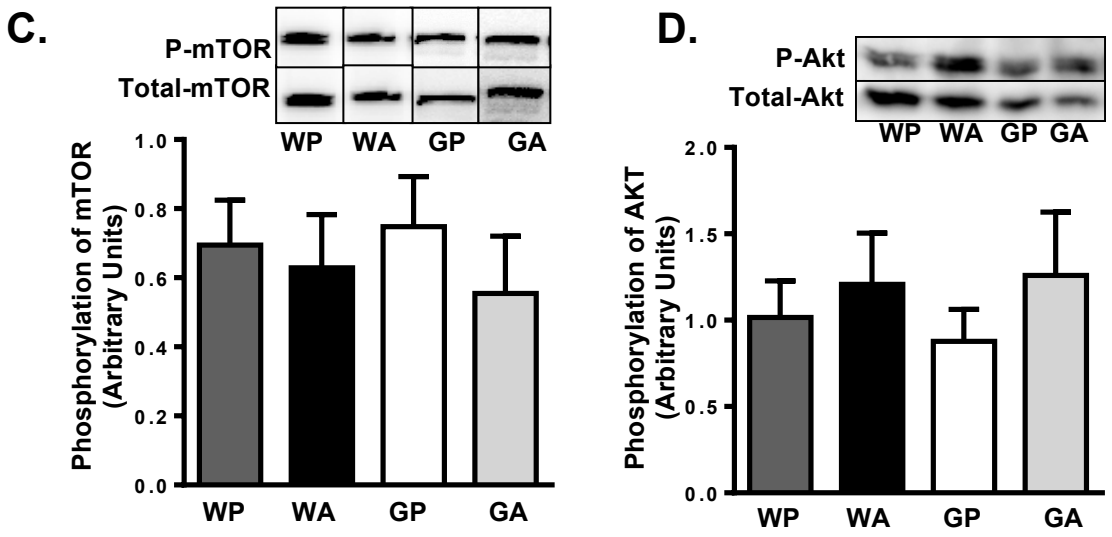


**Figure 14:** Treatment with asparaginase does not disrupt mTOR signaling pathway. **C:** Phosphorylation of mTOR at the serine 2448 site normalized for total mTOR measured by immunoblot (n=6 per group) **D:** Phosphorylation of Akt at the serine 473 phosphorylation site normalized for total Akt measured by immunoblot (n=6 per group). Animals were 8 week old, pure genetic background mice which received 8 IP injections of treatment. Mice were pair fed to the GCN2KO treated with asparaginase Values are means and error bars indicate SEM. X-axis represents treatment groups. Labeled means without a common letter were significantly different (P=0.05). WP, wild-type mice treated with PBS; WA, wild-type mice treated with asparaginase; GP, Gcn2 null mice treated with PBS; GA, Gcn2 null mice treated with asparaginase.

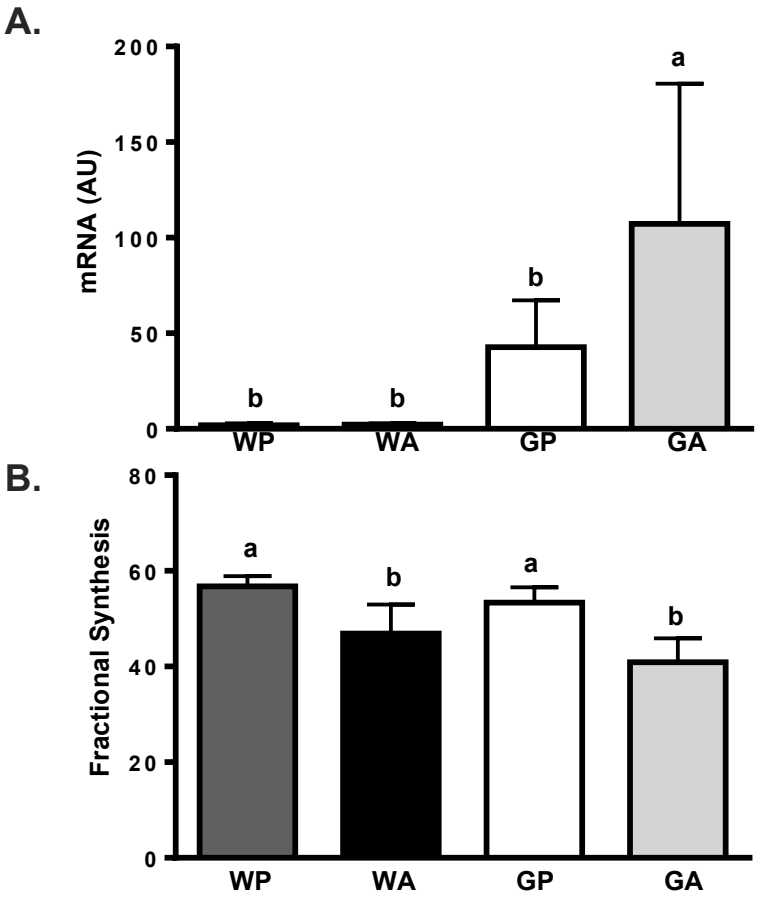


**Figure 15:** Evidence of Hepatic Stress **A:** Pancreatitis associated protein (PAP) mRNA expression increased in the liver of GA mice only. Hepatic PAP mRNA expression was determined by quantitative real-time PCR. AU=arbitrary units **B:** Liver protein synthesis is decreased by treatment with asparaginase. Fractional Synthesis Rate (FSR) of liver protein synthesis in 8 week old mixed genetic background mice following 8 IP injections of treatment (n=6 per group). Values are means and error bars indicate SEM. X-axis represents treatment groups. Labeled means without a common letter were significantly different (P=0.05). WP, wild-type mice treated with PBS; WA, wild-type mice treated with asparaginase; GP, Gcn2 null mice treated with PBS; GA, Gcn2 null mice treated with asparaginase.

| | WP | WA | GP | GA |
|---|---|---|---|---|
| **Asp** | 160.42 ± 23.09 | 163.67 ± 52.59 | 168.57 ± 36.87 | 157.80 ± 70.50 |
| **Glu** | 61.33 ± 8.71 [b] | 550.02 ± 204.52 [a] | 68.77 ± 22.99 [b] | 505.52 ± 329.33 [a] |
| **Asn** | 61.36 ±14.53 [a] | BDL [c] | 46.75 ± 7.42 [b] | BDL [c] |
| **Gln** | 452.75 ± 44.24 [a] | 177.29 ± 24.34 [b] | 400.26 ± 71.59 [a] | 147.66 ± 84.35 [b] |

**Supplemental Figure 1:** Serum amino acid levels of aspartic acid (asp), glutamic acid (glu), asparagine (asn) and glutamine (gln) 8 hours after intraperitoneal injection of asparaginase. Animals were 8 week old, pure genetic background mice which received 8 IP injections of treatment. Values are means±SEM, n=6 per group. BDL, below detection limits. Labeled means without a common letter were significantly different (P=0.05). WP, wild-type mice+PBS; WA, wild-type mice+asparaginase; GP, $Gcn2^{-/-}$mice+PBS; GA, $Gcn2^{-/-}$ mice+ asparaginase.

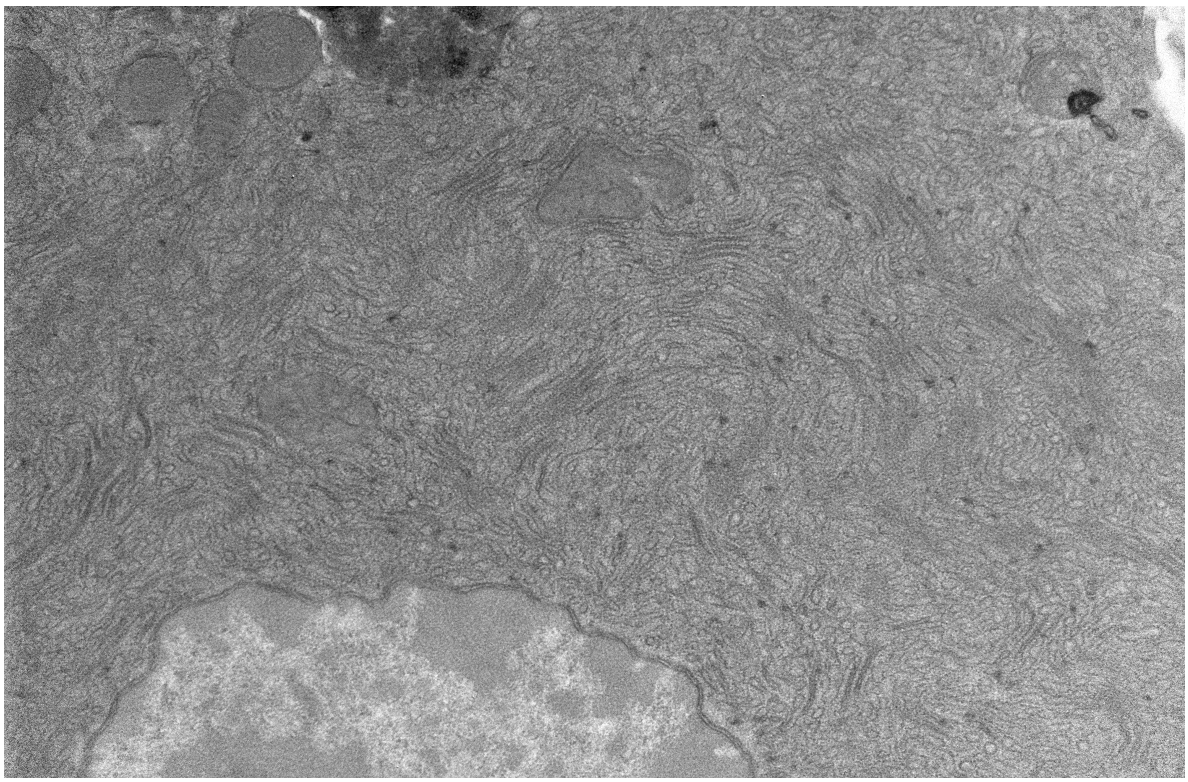

**Supplemental Figure 2:** Electron microscopy image of GCN2-/- animal treated with asparaginase. Visible disruption to endoplasmic reticulum and ragged nucleus.

# DISCUSSION

This study describes the role of GCN2 in the pancreas and the ability of this eIF2 kinase to promote cellular adaptation during asparaginase treatment. We observed that 1. Loss of GCN2 does not allow for activation of the AAR during enzymatic depletion of amino acids by asparaginase, leading to ER stress in the pancreas 2. Loss of GCN2 within the pancreas resulted in an increase in organ mass, which correlated with gene expression markers of inflammation and increased DNA damage 3. Pancreatic injury may be secondary to liver dysfunction in $GCN2^{-/-}$ mice treated with asparaginase. The results of these experiments have demonstrated how a functional defect in the critical eIF2 kinase stress pathway may predispose patients with ALL towards adverse metabolic events under chemotherapy treatment with asparaginase.

The pancreata of $GCN2^{-/-}$ mice treated with asparaginase showed signs of UPR activation both histologically and biochemically. From a histological perspective, we observed enlarged acinar cells and increased number of zymogen granules suggesting increased ER stress. Cerulein administration is a known model of pancreatitis and causes disruption by hyperstimulation of pancreatic acinar cells (86) leading to the accumulation of secretory proteins within the pancreas (74). In a cerulein-induced model of pancreatitis, H&E staining showed similar acinar cell appearance as our $GCN2^{-/-}$ animals treated with asparaginase, supporting the hypothesis of ER stress (86). Sah et al used cerulein to induce chronic pancreatitis and showed upregulation of the

components of the UPR were sustained following cerulein administration (87). Similarly, this study showed upregulated gene expression of components of the UPR. PERK signaling through eIF2 caused an increase in ATF4 mRNA expression in GA mice. GA mice also expressed increased mRNA expression of ATF6, sXBP1, BiP and ATF3 further suggesting that in the absence of GCN2 and the inability to activate the AAR, UPR activation occurs in an attempt to alleviate the cellular stress associated with asparaginase treatment.

The pancreas experiences high levels of intracellular protein turnover due to its function as both an endocrine and exocrine gland. During events of cellular stress, the ER can easily become overwhelmed. Despite the absence of GCN2, this study showed activation of genes involved in alleviating amino acid stress and ER stress. Spliced XBP1 was highest in both GCN2 null treatment groups, and was not significantly different in the GP or GA group. The high levels of this spliced variant suggests that GCN2 deletion pre-disposes this tissue to ER stress at baseline, prior to drug treatment. Although CHOP and C/EBP levels were not significantly different between any of the treatment groups, this may be due to the early stages and development of AAP. Based on the time frame of administration of asparaginase, the early stages of pancreatitis could be due to the time point selected. Weng et al reported that mice with cerulein induced pancreatitis exhibit deficient CHOP presented with increased inflammatory cytokines such as TNFα and IL-6, increased serum amylase and lipase activity and increased pancreatic pathology when compared to wildtype mice (88). Furthermore, these $CHOP^{-/-}$ mice exhibited low levels of cellular apoptosis and

higher levels of necrosis (88). A possible explanation for the consistent levels of CHOP expressed in the current study may indicate the degree of severity of ER stress. Suyama et al examined the involvement of CHOP in the acceleration of pancreatitis and demonstrated early activation of the ER stress pathway following cerulein injection (89). We study also observed that in $CHOP^{-/-}$ mice, inflammation cascade and apoptosis was inhibited compared to $CHOP^{+/+}$ mice which exhibited increased caspase activation. Similar to the present study, Suyama et al showed increased BiP and XBP1 expressed with no difference in serum amylase or cell death measured by TUNEL (89). Collectively, these studies suggest that CHOP induced apoptosis can reduce the severity of pancreatitis in mice. Since we propose that pancreatic injury is secondary to hepatic injury following asparaginase treatment, the degree of insult and ER stress to the pancreas may not rise high enough to elicit an increase in CHOP expression.

We also observed evidence of ER stress in $GCN2^{-/-}$ treated with asparaginase, however a bimodal distribution of gene expression was required in order to detail these findings. Indeed, not all animals in the GA group had begun to experience severe ER stress at day 8. Previously we reported that assigning GA mice to 14 days of asparaginase resulted in severe morbidity that required euthanasia between days 9-12 (48). Based on this, we anticipate continued treatment for longer than 8 days would elicit the UPR in all GA mice. Future studies require a more detailed time course evaluation to confirm this suggestion.

Pancreatic injury to acinar cells can occur through both apoptotic and necrotic mechanisms (90). Increased severity of acute pancreatitis is associated with necrosis of acinar cells, whereas mild acute pancreatitis is associated with apoptosis of acinar cells (88,90,83). Gukovskaya et al examined the role of TNFα in promoting apoptosis in acinar cells and reported that TNFα is localized in rat pancreatic acinar cells where it both produced and secreted (83). Additionally, this group reported an up-regulation of TNFα receptors during cerulein induced pancreatitis (83) suggesting that TNFα may an important signal in promoting inflammation leading to acinar cell death. The current study reported increased TNFα mRNA expression in the pancreas of GA mice, supporting the hypothesis that all GA mice would develop AAP and exhibit increased acinar cell death with prolonged asparaginase treatment.

In this study, we observed down regulation of the mTOR pathway in both wildtype and knockout animals following asparaginase treatment. Although data was not statistically significant, a similar trend of down regulation of this pathway was observed within the pancreas following a single asparaginase injection (27). Reinert et al showed a repression of signaling downstream of mTOR with a decrease in the phosphorylation of both 4EBP1 and S6K1 in the pancreas following a single injection with *E.coli* derived asparaginase (15). Future studies examining pancreatic protein synthesis would be relevant to examine the relative impact of mTORC1 versus the UPR in regulating protein synthesis rates in the pancreas.

In addition to the observation of decline of pancreatic health during

asparaginase treatment, is the concurrent development of diabetes. Patients reportedly exhibit medication induced diabetes (MID) and glucose intolerance during asparaginase treatment (91,92) These complications in regulating glucose following chemotherapy with asparaginase (91) may be due to ER stress in the pancreas following asparaginase treatment. Data shows that ER stress causes beta cell death in the pancreas (33) and that PERK deficient mice experience beta cell death, hyperglycemia and pancreatic hypoplasia (93,94) due to the inability to activate all three branches of the UPR. Additionally, glucose mediated insulin biosynthesis was significantly greater in the islets of PERK deficient mice than in islets of wild type animals (63). This suggests that activation of the UPR controls the rate of translation in response to glucose-mediated signals that otherwise promote insulin synthesis, and thus is critical for maintaining stress levels within the ER. Here we observed evidence of ER stress in the absence of GCN2. Thus, UPR activation and increased ER stressed observed in this study may be a conserved response in patients receiving asparaginase treatment that develop MID. A better understanding of the role of PERK activation during asparaginase treatment is important to better understand the mechanism of adverse metabolic events associated with asparaginase treatment and providing additional patient treatment options

Despite a decrease in body mass and an increase in pancreas size in GCN2$^{-/-}$ animals treated with asparaginase, we were unable to confirm the presence of pancreatitis using the clinical markers of pancreatitis. Our findings correspond to what is observed in the clinic (5,8,9,23,95); initial pancreatic

enzyme levels during the first 24-48 hours of symptoms are within the normal range before they become elevated in the blood (96). Additionally, several case studies indicate normal serum amylase levels persist for several weeks despite physical symptoms of pancreatitis (95,97,98). A 5-year retrospective study examining the onset of AAP reported that many patients manifested with clinical symptoms of pancreatitis and displayed low levels of pancreatic enzymes, yet these patients received a formal diagnosis of pancreatitis (7). Furthermore, if the animals in the present study had received treatment for more than 8 days, we would anticipate higher amylase activity in the GA treatment group. The decision to treat for 8 days was based on previous work performed in this lab. Wilson et al 2015 studied the effects of asparaginase treatment on the liver following 14 IP injections, however, none of the GA treated mice survived past day 12 (49). The present study was designed with 8 days of IP injections in order to study the onset of cellular dysfunction as opposed to studying cell death. Future studies examining serum lipase or elastase-1 to predict AAP could be beneficial in confirming pancreatitis.

Histological examination of the pancreas varied between wild-type and GCN2 knockout animals. In liver, asparaginase treatment increased lipid accumulation (49), however this was not the mechanism observed in the pancreas. In the pancreas, asparaginase reduced lipid content, visualized by Oil Red O, indicating that the increase in pancreas mass observed in the $GCN2^{-/-}$ mice treated with asparaginase was not due to lipid accumulation. Similarly, TUNEL staining in the liver showed increased DNA damage following

asparaginase treatment, with the most severe damage occurring in GCN2$^{-/-}$ livers treated with asparaginase (48). In the present study, we did not observe any differences in DNA damage visualized via TUNEL assay in the pancreas. This may have been due to the method of tissue preparation. The pancreas contains many ribonucleases, proteases and digestive enzymes which allow this tissue to aid in digestion (75) and function as an endocrine and exocrine organ. Because of this primary function of the pancreas, this tissue is highly active until it is completely frozen in liquid nitrogen following dissection from the animal. Due to the highly degradative nature of this tissue, the time between sacrifice and flash freezing may have allowed for cell death across all treatment groups. Future studies performing TUNEL on frozen sections of pancreas that are immersed in an RNAase inhibitor before fixation may help clarify the amount of cell death produced by drug versus gene deletion. Additionally, it appears as though both GCN2$^{-/-}$ treatment groups have fewer cells in the field of view. This may be due to the increased spacing between cells as confirmed by H&E staining. The decreased cell density of these two treatment groups could explain why there was no increase in cell death observed by TUNEL assay in the GA treatment group as expected. Future studies examining specifically examining cell death are needed for further clarification.

Studies have shown that FGF21 is rapidly expressed in models of *in vivo* pancreatitis (35,77) and that FGF21 plays a critical role in alleviating ER stress (99) and that the expression of FGF21 serves as an indicator of stress adaptation. Johnson et al showed that FGF21 expression was transiently

increased following injections of L-arginine, cerulein and CCK (77) showing multiple models of pancreatitis activate FGF21. Since one of the primary functions of the FGF family is to serve a protective role and in the current study, only the GCN2$^{-/-}$ animals treated with asparaginase expressed increased FGF21 mRNA levels, we propose that the presence of FGF21 is indicative of the cell trying to adapt to pancreatic injury. Furthermore, FGF21 is up-regulated in times of ER stress via a PERK-eIF2-ATF4 dependent cascade (99). Kim et al showed that FGF21 expression was increased in hepatocytes treated with tunicamycin concomitantly with other UPR genes including sXBP1, BiP and CHOP(99). Additionally, this study showed that FGF21 induction was suppressed in Perk$^{-/-}$ MEFs and that FGF21 expression was also attenuated in both eIF2α$^{-/-}$ and ATF4$^{-/-}$ MEFs (99) suggesting that the presence of this hormone is due to ER stress activation. Our data suggests GA mice suffer ER stress in response to asparaginase treatment and in an attempt to adapt to this stress phosphorylation of PERK and downstream signaling through ATF4 are responsible for the increase in FGF21 mRNA expression in the pancreas.

The alteration of lipid metabolism and cell death within the liver following asparaginase treatment suggests that pancreatic injury may be secondary to liver dysfunction. The concept of injury to the pancreas being secondary to injury in the liver is supported by intracellular concentrations of amino acids. We previously published that 1, 3 and 6 hours following asparaginase injections, asparagine and glutamine concentrations decreased in both liver and spleen, but remained constant in the pancreas (15). Since the secondary glutaminase

activity that occurs with asparaginase treatment is responsible for the adverse toxicities that follow, the unaltered amino acid concentrations provide additional support that the primary action of asparaginase occurs in the liver, and that complications seen in the pancreas are secondary to those in the liver.

Furthermore, phosphorylation of eIF2 following a single injection with asparaginase, increased with dose in the liver, but did not change in intensity in the pancreas despite the increasing dose (15). In the present study, there was no difference in phosphorylation of eIF2 in any of the treatment groups following 8 IP injections. This data agrees with previously published data in the pancreas. Following a single injection of asparaginase phosphorylation of eIF2 remained stable (27). The lack of difference in eIF2 phosphorylation suggests either basal levels of eIF2 phosphorylation are too high to reveal differences with stress, or an alternative kinase/pathway is being activated in this tissue to adapt to the stress under asparaginase treatment. Previous studies have shown high phosphorylation of eIF2 under non-stressful situations within the pancreas (100). PERK is most abundantly expressed in the pancreas (2,100–102) and may be responsible for the equal phosphorylation of eIF2 in our four treatment groups. Furthermore, the pancreas appears to be less stressed than liver, further suggesting the liver as the primary site of toxicity during asparaginase treatment.

We previously examined whether the supplementation of dietary glutamine in mice could alleviate the immunosuppressive effect of asparaginase due to its secondary glutamine depletion. Mice were given water or water supplemented with an alanyl-glutamine dipeptide in addition to receiving 7 IP

injections of asparaginase (103). This study found that although asparaginase depleted lymphocytes in bone marrow, spleen and thymus, the dietary supplementation of glutamine lessened the intensity of eIF2 phosphorylation in the spleen (103). This was an important discovery regarding the health benefits of dietary glutamine supplementation during asparaginase treatment. Future studies examining whether replacing glutamine levels would be beneficial to alleviate toxicities within the pancreas are necessary.

Our laboratory has previously shown that mice with a deletion of GCN2 following amino acid deprivation experienced adverse toxicity (15,27,48,49,69,72). Wildtype mice and GCN2 null mice received either a nutritionally adequate diet, or a diet lacking either leucine or glycine (69). $GCN2^{+/+}$ on the leucine deficient diet showed decreased body weight and liver weight, but were otherwise normal. However, many of the $GCN2^{-/-}$ mice on the leucine deficient diet died within 6 days of starting the diet (69). This study showed that defective GCN2 signaling and deprivation of a single amino acid has deleterious effects on the organism. Thus we presume that treating humans with asparaginase and the associated toxicities that follow, may be related to a defect somewhere within the GCN2/eIF2/ATF4 pathway. Under normal, nonstressed conditions, humans with a defect in GCN2 would not experience any side effects, given that western societies are typically well fed and do not suffer from amino acid insufficiencies. According to NCBI AceView, there are over 779 SNP mutations in the human gene of GCN2 known as EIF2AK4. This suggests there are many common mutations, which can affect function of GCN2, but in the

normally fed population these phenotypes are not observed. Thus these defects may be present in a portion of the population, however, based on our data, these defects would be inactive unless the organism found itself in a situation of amino acid deprivation.

Future research aimed at studying human samples for defects within eIF2 kinase stress pathways, would allow physicians to determine more accurately whether or not to use asparaginase during treatment of ALL. Identification of biological markers of these defects would help to inform physicians of patients harboring silent potential inabilities to handle the stress associated with asparaginase treatment. This would allow identified at risk patients to be treated with more tolerable therapies given their specific mutation. Additionally, having screened patients to see if this form of chemotherapy is compatible, there is an opportunity to develop new approaches to treatment such as synthetic kinases that could be delivered to the patient through adeno or AAV or other viral or vector therapeutic approaches.

An important follow up to this study would be to examine glucose homeostasis during asparaginase. Based on the literature, we would predict that mice that have an intact GCN2 and receive asparaginase injections would have normal glucose and insulin levels, whereas $GCN2^{-/-}$ mice treated with asparaginase would show evidence of glucose disregulation. The present study provides evidence of the mechanism behind MID during asparaginase treatment. Patients with a defect in in GCN2 would be unable to fully activate the AAR, which may be followed by increased ER stress as we have currently shown.

Future animal studies measuring glucose and insulin are necessary to further elucidate this disregulation. Additionally, the use of electron microscopy to visualize changes in pancreatic organization following asparaginase treatment would be helpful to confirm our molecular findings of ER stress.

Another important follow up study would be to determine the cause of the increased pancreas mass observed following asparaginase treatment. This study showed that when expressed as a percentage of body weight, the $GCN2^{-/-}$ mice treated with asparaginase had the largest pancreas mass relative to body size. This study also showed with H&E staining that at baseline, there are fundamental differences between $GCN2^{+/+}$ and $GCN2^{-/-}$ pancreas. Specifically, the $GCN2^{-/-}$ animals appear to have increased space in between cells. We hypothesize that the increase in pancreas mass may be due to fluid accumulation with these spaces. Examining the dry verses wet weight of the pancreas is important to determine if the increase in pancreas mass is due to excess fluid accumulation.

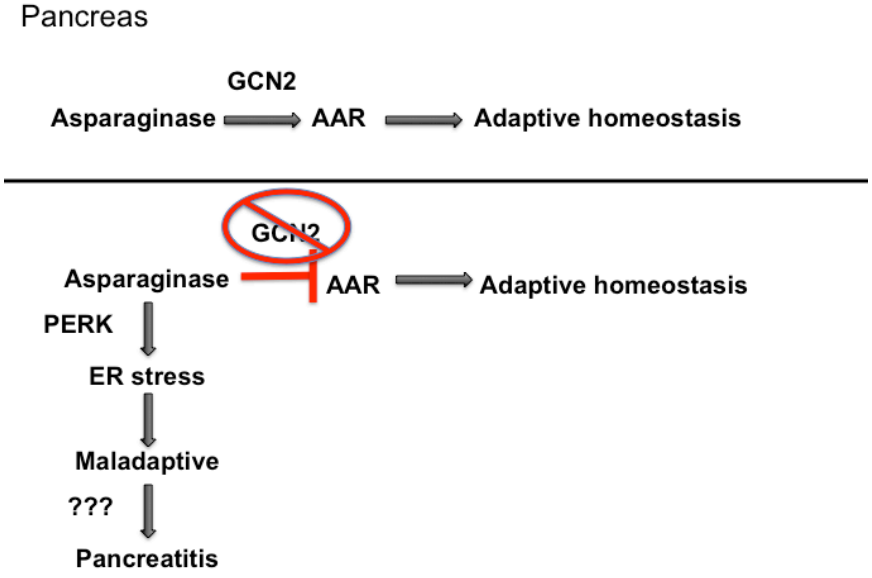

**Figure 16:** Summary of pancreatic dysfunction during asparaginase treatment. Top: adaptive recovery due to the presence of intact GCN2. Bottom: Pancreatitis associated with the absence of functional GCN2.

The majority of related current studies focus on drug treatment options for patients suffering from AAP. These studies are predominantly retrospective and examine how additional drugs can be used in combination with asparaginase to prevent some of the toxic side effects. Previously, we did not understand the precise mechanism of drug action on a cellular level and how the depletion of normally non-essential amino acids affects the whole body. The concept that GCN2 deficiency promotes AAP provides important insight into improving options for patient treatment. Furthermore, the importance of GCN2 in modulating the wide array of side effects seen by chemotherapy with asparaginase may relate to inherent insufficiency of this stress pathway in patients.

# REFERENCES


1. Flores-Calderon, J., Exiqa-Gonzalez, E., Moran-Villota, S., Martin-Trejo, J., Yamamoto-Nagano A. Acute Pancreatitis in children with acute lymphoblastic leukemia treated with L-asparaginase. J Pediatr Hematol Oncol. 1994;296–7.

2. Wek RC, Jiang H-Y, Anthony TG. Coping with stress: eIF2 kinases and translational control. Biochem Soc Trans. 2006;7–11.

3. Sattar HA. Fundamentals of Pathology: Medical Course and Step 1 Review. 2011. 218 p.

4. National Cancer Institute.

5. Raja RA, Schmiegelow K, Frandsen TL. Asparaginase-associated pancreatitis in children. British Journal of Haematology. 2012. p. 18–27.

6. Dufour E, Gay F, Aguera K, Scoazec J-Y, Horand F, Lorenzi PL, Godfrin Y. Pancreatic Tumor Sensitivity to Plasma L-Asparagine Starvation. Pancreas. 2012. p. 940–8.

7. Knoderer HM, Robarge J, Flockhart DA. Predicting asparaginase-associated pancreatitis. Pediatr Blood Cancer. 2007;634–9.

8. Treepongkaruna S, Thongpak N, Pakakasama S, Pienvichit P, Sirachainan N, Hongeng S. Acute Pancreatitis in Children With Acute Lymphoblastic Leukemia After Chemotherapy. Journal of Pediatric Hematology/Oncology. 2009. p. 812–5.

9. Muwakkit S, Saab R, Yazbeck N, Samia L, Abboud MR. L-asparaginase-induced pancreatitis in children with acute lymphoblastic leukemia: is allopurinol protective? Pediatr Hematol Oncol. 2010;496–501.

10. Leslie M, Case MC, Hall AG, Coulthard SA. Expression levels of asparagine synthetase in blasts from children and adults with acute lymphoblastic leukaemia. Br J Haematol. 2006;740–2.

11. Aslanian AM, Fletcher BS, Kilberg MS. Asparagine synthetase expression alone is sufficient to induce l-asparaginase resistance in MOLT-4 human leukaemia cells. Biochem J. 2001;321–8.

12. Broome BYJD. STUDIES ON THE MECHANISM OF TUMOR INHIBITION BY L-ASPARAGINASE The identification of L-asparaginase as the

constituent of guinea pig serum responsible for its tumor-inhibitory properties is now generally accept. 1968;1055–72.

13. El-Nagga NE-A, El-Ewasy SM, El-Shweihy NM. Microbial L-asparaginase as a Potential Therapeutic Agent for the Treatment of Acute Lymphoblastic Leukemia: The Pros and Cons. Int J Pharmacol. 2014;182–99.

14. Ollenschläger G, Roth E, Linkesch W, Jansen S, Simmel a, Mödder B. Asparaginase-induced derangements of glutamine metabolism: the pathogenetic basis for some drug-related side-effects. Eur J Clin Invest. 1988;512–6.

15. Reinert RB, Oberle LM, Wek SA, Bunpo P, Xue PW, Mileva I, Goodwin LO, Aldrich CJ, Durden DL, McNurlan MA, Wek RC, Anthony TG. Role of glutamine depletion in directing tissue-specific nutrient stress responses to L-asparaginase. J Biol Chem. 2006;31222–33.

16. Michael Rytting M. Role of L-asparaginase in acute lymphoblastic leukemia: focus on adult patients. Blood Lymphat Cancer Targets Ther. 2012;117.

17. Ramya LN, Doble M, Rekha VPB, Pulicherla KK. L-asparaginase as potent anti-leukemic agent and its significance of having reduced glutaminase side activity for better treatment of acute lymphoblastic leukaemia. Applied Biochemistry and Biotechnology. 2012. p. 2144–59.

18. Appel IM, Kazemier KM, Boos J, Lanvers C, Huijmans J, Veerman a JP, van Wering E, den Boer ML, Pieters R. Pharmacokinetic, pharmacodynamic and intracellular effects of PEG-asparaginase in newly diagnosed childhood acute lymphoblastic leukemia: results from a single agent window study. Leuk Off J Leuk Soc Am Leuk Res Fund, UK. 2008;1665–79.

19. Tong WH, Pieters R, Kaspers GJL, Te Loo DMWM, Bierings MB, Van Den Bos C, Kollen WJW, Hop WCJ, Lanvers-Kaminsky C, Relling M V., Tissing WJE, Van Der Sluis IM. A prospective study on drug monitoring of PEGasparaginase and Erwinia asparaginase and asparaginase antibodies in pediatric acute lymphoblastic leukemia. Blood. 2014;2026–33.

20. Müller HJ, Boos J. Use of L-asparaginase in childhood ALL. Critical Reviews in Oncology/Hematology. 1998. p. 97–113.

21. Masetti R, Pession A. First-line treatment of acute lymphoblastic leukemia with pegasparaginase. Biologics. 2009;359–68.

22. Avramis VI, Tiwari PN. Asparaginase (native ASNase or pegylated ASNase) in the treatment of acute lymphoblastic leukemia. International Journal of Nanomedicine. 2006. p. 241–54.

23. Raja R a., Schmiegelow K, Albertsen BK, Prunsild K, Zeller B, Vaitkeviciene G, Abrahamsson J, Heyman M, Taskinen M, Harila-Saari A, Kanerva J, Frandsen TL. Asparaginase-associated pancreatitis in children with acute lymphoblastic leukaemia in the NOPHO ALL2008 protocol. Br J Haematol. 2014;126–33.

24. Dores GM, Devesa SS, Curtis RE, Linet MS, Morton LM. Acute leukemia incidence and patient survival among children and adults in the United States, 2001-2007. Blood. 2011;34–43.

25. Balasubramanian MN, Butterworth E a, Kilberg MS. Asparagine synthetase: regulation by cell stress and involvement in tumor biology. Am J Physiol Endocrinol Metab. 2013;E789–99.

26. Sood R, Porter AC, Olsen D, Cavener DR, Wek RC. A mammalian homologue of GCN2 protein kinase important for translational control by phosphorylation of eukaryotic initiation factor-2α Genetics. 2000;787–801.

27. Bunpo P, Dudley A, Cundiff JK, Cavener DR, Wek RC, Anthony TG. GCN2 protein kinase is required to activate amino acid deprivation responses in mice treated with the anti-cancer agent L-asparaginase. J Biol Chem. 2009;32742–9.

28. Qiu H, Dong J, Hu C, Francklyn CS, Hinnebusch AG. The tRNA-binding moiety in GCN2 contains a dimerization domain that interacts with the kinase domain and is required for tRNA binding and kinase activation. EMBO J. 2001;1425–38.

29. Visweswaraiah J, Lageix S, Castilho B a., Izotova L, Kinzy TG, Hinnebusch AG, Sattlegger E. Evidence that eukaryotic translation elongation factor 1A (eEF1A) binds the Gcn2 protein C terminus and inhibits Gcn2 activity. J Biol Chem. 2011;36568–79.

30. Yamaguchi S, Ishihara H, Yamada T, Tamura A, Usui M, Tominaga R, Munakata Y, Satake C, Katagiri H, Tashiro F, Aburatani H, Tsukiyama-Kohara K, Miyazaki J, Sonenberg N, Oka Y. ATF4-mediated induction of 4E-BP1 contributes to pancreatic beta cell survival under endoplasmic reticulum stress. Cell Metab. 2008;269–76.

31. Sans MD, Lee S-H, D'Alecy LG, Williams JA. Feeding activates protein synthesis in mouse pancreas at the translational level without increase in mRNA. Am J Physiol Gastrointest Liver Physiol. 2004;G667–75.

32. Harding HP, Zhang Y, Zeng H, Novoa I, Lu PD, Calfon M, Sadri N, Yun C, Popko B, Paules R, Stojdl DF, Bell JC, Hettmann T, Leiden JM, Ron D. An integrated stress response regulates amino acid metabolism and resistance to oxidative stress. Mol Cell. 2003;619–33.

33. Eizirik DL, Miani M, Cardozo AK. Signalling danger: Endoplasmic reticulum stress and the unfolded protein response in pancreatic islet inflammation. Diabetologia. 2013. p. 234–41.

34. Su, NanSu, N., & Kilberg, M. S. C/EBP homology protein (CHOP) interacts with activating transcription factor 4 (ATF4) and negatively regulates the stress-dependent induction of the asparagine synthetase gene. J Biol Chem. 2008;35106–17.

35. Kim KH, Lee M. FGF21 as a Stress Hormone : The Roles of FGF21 in Stress Adaptation and the Treatment of Metabolic Diseases. 2014;245–51.

36. Rydén M. Fibroblast growth factor 21: an overview from a clinical perspective. Cell Mol Life Sci. 2009;2067–73.

37. So WY, Cheng Q, Chen L, Evans-Molina C, Xu A, Lam KSL, Leung PS. High glucose represses β-klotho expression and impairs fibroblast growth factor 21 action in mouse pancreatic islets: Involvement of peroxisome proliferator-activated receptor γ signaling. Diabetes. 2013;3751–9.

38. Badman MK, Pissios P, Kennedy AR, Koukos G, Flier JS, Maratos-Flier E. Hepatic Fibroblast Growth Factor 21 Is Regulated by PPARγ and Is a Key Mediator of Hepatic Lipid Metabolism in Ketotic States. Cell Metab. 2007;426–37.

39. Kharitonenkov A, Shiyanova TL, Koester A, Ford AM, Micanovic R, Galbreath EJ, Sandusky GE, Hammond LJ, Moyers JS, Owens RA, Gromada J, Brozinick JT, Hawkins ED, Wroblewski VJ, Li DS, Mehrbod F, Jaskunas SR, Shanafelt AB. FGF-21 as a novel metabolic regulator. J Clin Invest. 2005;1627–35.

40. Wente W, Efanov AM, Brenner M, Kharitonenkov A, Köster A, Sandusky GE, Sewing S, Treinies I, Zitzer H, Gromada J. Fibroblast growth factor-21 improves pancreatic beta-cell function and survival by activation of extracellular signal-regulated kinase 1/2 and Akt signaling pathways. Diabetes. 2006;2470–8.

41. Laplante M, Sabatini DM. mTOR signaling. Cold Spring Harb Perspect Biol. 2012;2009–11.

42. Laplante M, Sabatini DM. Regulation of mTORC1 and its impact on gene expression at a glance. J Cell Sci. 2013;1713–9.

43. Bar-Peled L, Sabatini DM. Regulation of mTORC1 by amino acids. Trends Cell Biol. 2014;400–6.

44. Moody C a, Scott RS, Amirghahari N, Nathan C, Young LS, Dawson CW, Sixbey JW. Modulation of the Cell Growth Regulator mTOR by Epstein-Barr. Society. 2005;5499–506.

45. Dann SG, Thomas G. The amino acid sensitive TOR pathway from yeast to mammals. FEBS Lett. 2006;2821–9.

46. Dennis MD, Jefferson LS, Kimball SR. Role of p70S6K1-mediated phosphorylation of eIF4B and PDCD4 proteins in the regulation of protein synthesis. J Biol Chem. 2012;42890–9.

47. Kim YC, Guan K. mTOR : a pharmacologic target for autophagy regulation. 2015;25–32.

48. Wilson GJ, Bunpo P, Cundiff JK, Wek RC, Anthony TG. The eukaryotic initiation factor 2 kinase GCN2 protects against hepatotoxicity during asparaginase treatment. Am J Physiol Endocrinol Metab. 2013;E1124–33.

49. Wilson GJ, Lennox B a., She P, Mirek ET, Al Baghdadi RJT, Fusakio ME, Dixon JL, Henderson GC, Wek RC, Anthony TG. GCN2 is required to increase fibroblast growth factor 21 and maintain hepatic triglyceride homeostasis during asparaginase treatment. Am J Physiol - Endocrinol Metab. 2015;E283–93.

50. Julier, Cecile. Nicolino M. Wolcott-Rallison syndrome. Orphanet J Rare Dis. BioMed Central Ltd; 2010;2–13.

51. Hotamisligil GS. Endoplasmic Reticulum Stress and the Inflammatory Basis of Metabolic Disease. Cell. 2010. p. 900–17.

52. Schröder M, Kaufman RJ. The mammalian unfolded protein response. Annu Rev Biochem. 2005;739–89.

53. Hoseki J, Ushioda R, Nagata K. Mechanism and components of endoplasmic reticulum-associated degradation. Journal of Biochemistry. 2010. p. 19–25.

54. Kaser A, Flak MB, Tomczak MF, Blumberg RS. The unfolded protein response and its role in intestinal homeostasis and inflammation. Exp Cell Res. Elsevier Inc.; 2011;2772–9.

55. Shen J, Chen X, Hendershot L, Prywes R. ER stress regulation of ATF6 localization by dissociation of BiP/GRP78 binding and unmasking of golgi localization signals. Dev Cell. 2002;99–111.

56. Vattem KM, Wek RC. Reinitiation involving upstream ORFs regulates ATF4 mRNA translation in mammalian cells. Proc Natl Acad Sci U S A. 2004;11269–74.

57. Kober L, Zehe C, Bode J. Development of a Novel ER Stress Based Selection System for the Isolation of Highly Productive Clones. 2012;2599–611.

58. Yoshida H, Matsui T, Yamamoto A, Okada T, Mori K. XBP1 mRNA is induced by ATF6 and spliced by IRE1 in response to ER stress to produce a highly active transcription factor. Cell. 2001;881–91.

59. Lee K, Tirasophon W, Shen X, Michalak M, Prywes R, Okada T, Yoshida H, Mori K, Kaufman RJ. IRE1-mediated unconventional mRNA splicing and S2P-mediated ATF6 cleavage merge to regulate XBP1 in signaling the unfolded protein response. Genes Dev. 2002;452–66.

60. Chen X, Shen J, Prywes R. The luminal domain of ATF6 senses endoplasmic reticulum (ER) stress and causes translocation of ATF6 from the er to the Golgi. J Biol Chem. 2002;13045–52.

61. Xu C, Bailly-Maitre B, Reed J. Endoplasmic reticulum stress: cell life and death decisions. J Clin Invest. 2005;2656–64.

62. Efeyan A, Comb WC, Sabatini DM. Nutrient-sensing mechanisms and pathways. Nature. 2015;997–1003.

63. Harding HP, Zeng H, Zhang Y, Jungries R, Chung P, Plesken H, Sabatini DD, Ron D. Diabetes mellitus and exocrine pancreatic dysfunction in Perk-/- mice reveals a role for translational control in secretory cell survival. Mol Cell. 2001;1153–63.

64. Pictet RL, Clark WR, Williams RH, Rutter WJ. An ultrastructural analysis of the developing embryonic pancreas. Dev Biol. 1972;436–67.

65. Back SH, Kang S-W, Han J, Chung H-T. Endoplasmic Reticulum Stress in the β-Cell Pathogenesis of Type 2 Diabetes. Exp Diabetes Res. 2012;618396.

66. Volchuk a., Ron D. The endoplasmic reticulum stress response in the pancreatic β-cell. Diabetes, Obes Metab. 2010;48–57.

67. Herbert TP. PERK in the life and death of the pancreatic beta-cell. Biochem Soc Trans. 2007;1205–7.

68. Oyadomari S, Koizumi A, Takeda K, Gotoh T, Akira S, Araki E, Mori M. Targeted disruption of the Chop gene delays endoplasmic reticulum stress-mediated diabetes. J Clin Invest. 2002;525–32.

69. Anthony TG, McDaniel BJ, Byerley RL, McGrath BC, Cavener DB, McNurlan MA, Wek RC. Preservation of liver protein synthesis during dietary leucine deprivation occurs at the expense of skeletal muscle mass in mice deleted for eIF2 kinase GCN2. J Biol Chem. 2004;36553–61.

70. Guo F, Cavener DR. The GCN2 eIF2α Kinase Regulates Fatty-Acid Homeostasis in the Liver during Deprivation of an Essential Amino Acid. Cell Metab. 2007;103–14.

71. Hao S, Sharp JW, Ross-Inta CM, McDaniel BJ, Anthony TG, Wek RC, Cavener DR, McGrath BC, Rudell JB, Koehnle TJ, Gietzen DW. Uncharged tRNA and sensing of amino acid deficiency in mammalian piriform cortex. Science. 2005;1776–8.

72. Bunpo P, Cundiff JK, Reinert RB, Wek RC, Aldrich CJ, Anthony TG. The eIF2 kinase GCN2 is essential for the murine immune system to adapt to amino acid deprivation by asparaginase. J Nutr. 2010;2020–7.

73. Garlick PJ, McNurlan M a, Preedy VR. A rapid and convenient technique for measuring the rate of protein synthesis in tissues by injection of [3H]phenylalanine. Biochem J. 1980;719–23.

74. Mayerle J, Sendler M, Lerch MM. Secretagogue ( Caerulein ) induced pancreatitis in rodents. Medicine (Baltimore). 2013;

75. Azevedo-Pouly ACP, Elgamal O a., Schmittgen TD. RNA Isolation from Mouse Pancreas: A Ribonuclease-rich Tissue. J Vis Exp. 2014;2–7.

76. Roskoski R. ERK1/2 MAP kinases: Structure, function, and regulation. Pharmacol Res. Elsevier Ltd; 2012;105–43.

77. Johnson CL, Weston JY, Chadi S a., Fazio EN, Huff MW, Kharitonenkov A, Köester A, Pin CL. Fibroblast Growth Factor 21 Reduces the Severity of Cerulein-Induced Pancreatitis in Mice. Gastroenterology. Elsevier Inc.; 2009;1795–804.

78. Chiribau C-B, Gaccioli F, Huang CC, Yuan CL, Hatzoglou M. Molecular symbiosis of CHOP and C/EBP beta isoform LIP contributes to

endoplasmic reticulum stress-induced apoptosis. Mol Cell Biol. 2010;3722–31.

79. Kaufman RJ. Regulation of mRNA translation by protein folding in the endoplasmic reticulum. Trends in Biochemical Sciences. 2004. p. 152–8.

80. Pulido-Salgado M, Vidal-Taboada JM, Saura J. C/EBPβ and C/EBPδ transcription factors: Basic biology and roles in the CNS [Internet]. Progress in Neurobiology. 2015.

81. Yamaguchi K, Lee S-H, Kim J-S, Wimalasena J, Kitajima S, Baek SJ. Activating transcription factor 3 and early growth response 1 are the novel targets of LY294002 in a phosphatidylinositol 3-kinase-independent pathway. Cancer Res. 2006;

82. Kemppainen E, Sand J, Puolakkainen P, Laine S, Hedstrom J, Sainio V, Haapiainen R. Pancreatitis associated protein as an early marker of acute pancreatitis. 1996;675–8.

83. Gukovskaya a S, Gukovsky I, Zaninovic V, Song M, Sandoval D, Gukovsky S, Pandol SJ. Pancreatic acinar cells produce, release, and respond to tumor necrosis factor-alpha. Role in regulating cell death and pancreatitis. J Clin Invest. 1997;1853–62.

84. Pagel J-I, Deindl E. Early growth response 1--a transcription factor in the crossfire of signal transduction cascades. Indian J Biochem Biophys. 2011;

85. Gong LB, He L, Liu Y, Chen XQ, Jiang B. Expression of early growth response factor-1 in rats with cerulein-induced acute pancreatitis and its significance. World J Gastroenterol. 2005;

86. Jacob TG, Raghav R, Kumar A, Garg PK, Roy TS. Duration of injury correlates with necrosis in caerulein-induced experimental acute pancreatitis: implications for pathophysiology. Int J Exp Pathol. 2014;199–208.

87. Sah RP, Garg SK, Dixit AK, Dudeja V, Dawra RK, Saluja AK. Endoplasmic Reticulum stress is chronically activated in chronic pancreatitis. J Biol Chem. 2014;0–28.

88. Weng T-I. C/EBP homologous protein deficiency aggravates acute pancreatitis and associated lung injury. World J Gastroenterol. 2013;7097.

89. Suyama K, Ohmuraya M, Hirota M, Ozaki N, Ida S, Endo M, Araki K, Gotoh T, Baba H, Yamamura KI. C/EBP homologous protein is crucial for

the acceleration of experimental pancreatitis. Biochem Biophys Res Commun. 2008;176–82.

90. Bhatia M. Apoptosis versus necrosis in acute pancreatitis. Am J Physiol Gastrointest Liver Physiol. 2004;G189–96.

91. Bostrom B, Uppal P, Chu J, Messinger Y, Gandrud L, McEvoy R. Safety and efficacy of metformin for therapy-induced hyperglycemia in children with acute lymphoblastic leukemia. J Pediatr Hematol Oncol. 2013;504–8.

92. Koltin D, Sung L, Naqvi A, Urbach SL. Medication induced diabetes during induction in pediatric acute lymphoblastic leukemia: prevalence, risk factors and characteristics. Support Care Cancer. 2012;2009–15.

93. Scheuner D, Song B, McEwen E, Liu C, Laybutt R, Gillespie P, Saunders T, Bonner-Weir S, Kaufman RJ. Translational control is required for the unfolded protein response and in vivo glucose homeostasis. Mol Cell. 2001;1165–76.

94. Thornton CM, Carson DJ, Stewart FJ. Autopsy findings in the Wolcott-Rallison syndrome. Pediatric pathology & laboratory medicine : journal of the Society for Pediatric Pathology, affiliated with the International Paediatric Pathology Association. p. 487–96.

95. Alvarez O a., Zimmerman G. Pegaspargase-induced pancreatitis. Med Pediatr Oncol. 2000;200–5.

96. Oh HJ, Im SA, Lee JW, Chung NG, Cho B. Relationship Between Modified CT Severity Index and Clinical Features of L-Asparaginase-Associated Pancreatitis in Pediatric Acute Lymphoblastic Leukemia. Pediatr Hematol. 2014;647–55.

97. Morimoto T. Early diagnosis of asparaginase-associated pancreatitis based on elevated serum elastase-1 levels: Case reports. Biomed Reports. 2013;651–3.

98. Shimizu T, Yamashiro Y, Igarashi J, Fujita H, Ishimoto K. Increased serum trypsin and elastase-1 levels in patients undergoing L-asparaginase therapy. Eur J Pediatr. 1998;561–3.

99. Kim SH, Kim KH, Kim H, Kim M, Back SH, Konishi M. Fibroblast growth factor 21 participates in adaptation to endoplasmic reticulum stress and attenuates obesity-induced hepatic metabolic stress. 2014;

100. Zhang P, McGrath B, Li S, Frank A, Zambito F, Reinert J, Gannon M, Ma K, McNaughton K, Cavener DR. The PERK Eukaryotic Initiation Factor 2α

Kinase Is Required for the Development of the Skeletal System, Postnatal Growth, and the Function and Viability of the Pancreas. Mol Cell Biol. 2002;3864–74.

101. Shi Y, An J, Liang J, Hayes SE, Sandusky GE, Stramm LE, Yang NN. Characterization of a mutant pancreatic eIF-2alpha kinase, PEK, and co-localization with somatostatin in islet delta cells. J Biol Chem. 1999;5723–30.

102. Shi Y, Vattem KM, Sood R, An J, Liang J, Stramm L, Wek RC. Identification and characterization of pancreatic eukaryotic initiation factor 2 alpha-subunit kinase, PEK, involved in translational control. Mol Cell Biol. 1998;7499–509.

103. Bunpo P, Murray B, Cundiff J, Brizius E, Aldrich CJ, Anthony TG. Alanyl-glutamine consumption modifies the suppressive effect of L-asparaginase on lymphocyte populations in mice. J Nutr. 2008;338–43.